Journal of Nanomaterials

Carbon-Based Nanomaterials in Pest and Environmental Management

Lead Guest Editor: Seema Ramniwas
Guest Editors: Divya Singh, Pankaj Tyagi, and Girish Kumar

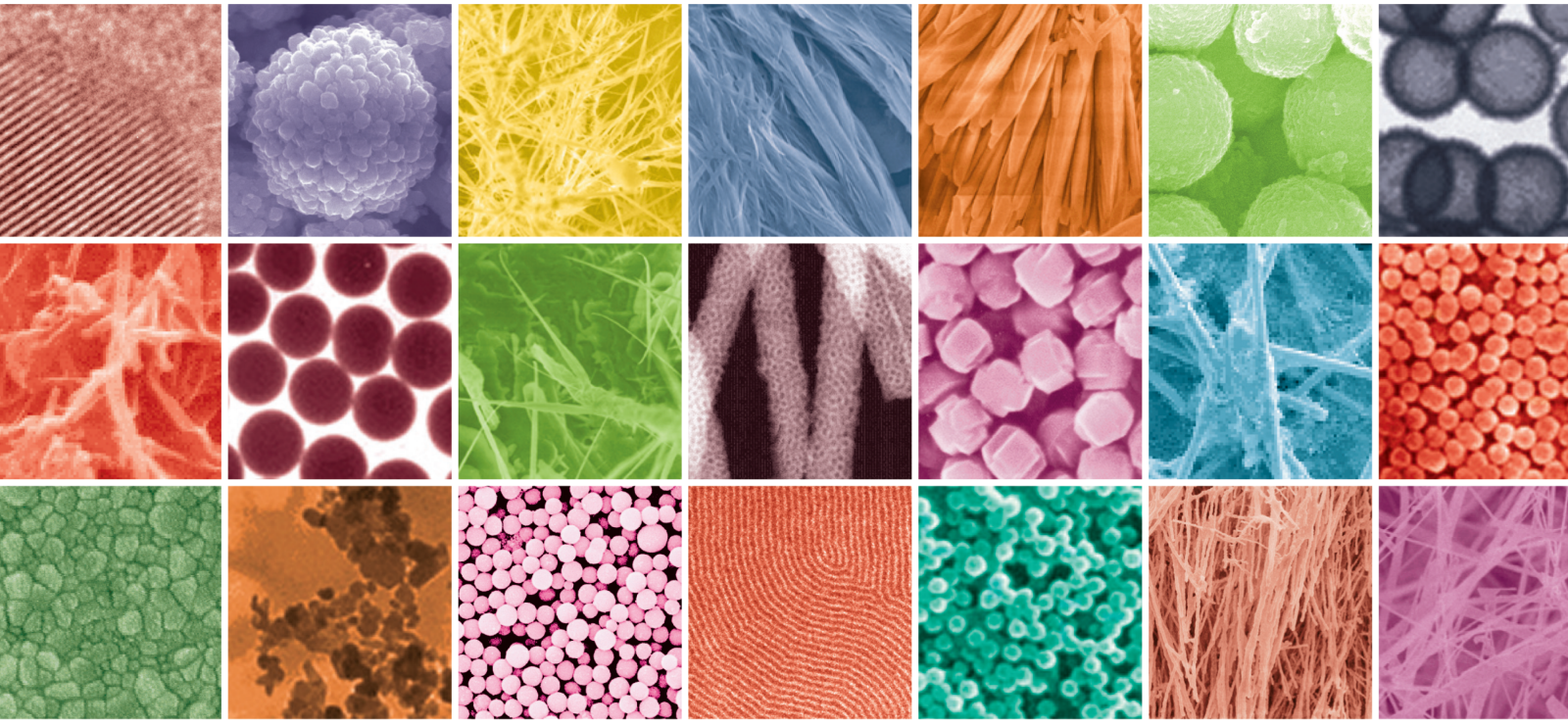

Carbon-Based Nanomaterials in Pest and Environmental Management

Journal of Nanomaterials

Carbon-Based Nanomaterials in Pest and Environmental Management

Lead Guest Editor: Seema Ramniwas
Guest Editors: Divya Singh, Pankaj Tyagi, and Girish Kumar

Contents

Hindawi
Journal of Nanomaterials
Volume 2023, Article ID 4703650, 11 pages
https://doi.org/10.1155/2023/4703650

Research Article

Bioactivity of Citral and Its Nanoparticle in Attenuating Pathogenicity of *Pseudomonas aeruginosa* and Controlling *Drosophila melanogaster*

Aanchal Sharma,[1] **Kusum Harjai**,[2] **Seema Ramniwas**,[1] **and Divya Singh**[1]

[1]*University Center for Research and Development, Chandigarh University, Mohali 140413, India*
[2]*Department of Microbiology, Panjab University, Sector 14, Chandigarh 160014, India*

Correspondence should be addressed to Seema Ramniwas; seema.ramniwas@gmail.com

Received 18 July 2022; Revised 1 October 2022; Accepted 19 October 2022; Published 23 January 2023

Academic Editor: Dong Kee Yi

Plant-based essential oils are hydrophobic, volatile concentrate extracted from aromatic plants. They are the upcoming alternative and appealing source of antimicrobial compounds, citral (major constituent of lemongrass oil) being one of them, whose anti-quorum sensing, in vivo delivery, and insecticidal potential need further exploration. *Pseudomonas aeruginosa* is one of the most prevalent, clinically lethal pathogens, which is resistible toward various treatments because of the inherent resistance acquired by the organism to many classes of drugs (multidrug resistant (MDR)). Moreover, fruit flies have been considered as the vectors of potentially lethal and opportunistic pathogens, including multiantibiotic-resistant microbes. As a result, controlling both the pathogen and its host vector are of utmost importance. The present study focused on the efficacy of essential oil of citral (EOC) and its nanoencapsulated form on quorum sensing inhibition (QSI) of *P. aeruginosa* PAO1 and its insecticidal activity against *Drosophila melanogaster*. Chitosan-based citral nanoparticles were synthesized and characterized using hydrodynamic size, zeta potential, polydispersity index, and field-emission scanning electron microscopy (FE-SEM). Citral nanoparticles at sub-minimum inhibitory concentration (MIC) exhibited QSI potential by attenuating biofilm formation (p-value < 0.05), while insecticidal activity of citral tested against *D. melanogaster* demonstrated toxicity of the EOC at a concentration of 3%–5%. Hence, the results elucidated the prospects of citral nanoparticles in the delivery of citral, which can be applied as a strategy to specifically target clinically lethal pathogens, major insect pests, and associated microbes.

1. Introduction

The present era of antibiotic resistance and sudden emergence of lethal human pathogens are due to the surfacing of multidrug-resistant (MDR) variants worldwide. *Pseudomonas aeruginosa* is one of the intractable pathogens, implicated in a number of lethal nosocomial infections, as the organism is inherently resistant to many classes of drugs, including cephalosporins, aminoglycosides, quinolones, and the carbapenems. Thus, the antibiotic-resistant variants are the main cause of a copious number of clinical infections associated with *P. aeruginosa*. The pathogenesis of the bacterium within the host involves the use of highly sophisticated genotypic events to bolster various molecular and phenotypic mechanisms that enable it to survive under antibiotic stress [1]. The pathogen achieves clinical irresistibility due to the presence of various virulence factors, which can be extracellular and/or intracellular. In addition to this, *P. aeruginosa* has another outstanding characteristic of forming planktonic and biofilm cells, which enable it to cause both acute and chronic infections. Bacteria create very persistent biofilm cells in tensible conditions, such as those found in cystic fibrosis-infected lungs and viscera, allowing it to live and endure for longer periods of time. Therefore, it is practically impossible to eradicate *P. aeruginosa* infections, which are mediated through the phenomenon of quorum sensing (QS) [2]. Hence, novel strategies need to be implemented that could potentially target the QS of *P. aeruginosa* populations and, hence, could attenuate its

pathogenicity in clinical settings rather than directly killing the pathogen.

The first QS system was elucidated in 1985 and since then, there have been a lot of discussion among researchers about the potential of attenuating the QS system of bacteria in order to restrain its pathogenesis. The quest for reliable QS antagonists has continued ever since, with researchers exploring natural plant-derived products with efficient activity and chemical stability in small doses. This has led to the emergence of new area of research exploration, namely, quorum quenching (QQ), which involves all the means by which QS system of bacteria could be attenuated or hindered. The attenuation of QS system by means of QQ could pay the way for alternate strategy to regulate population density and gene expression and, hence, pathogenesis of bacteria accordingly. The molecular determinants of QQ can be proteinaceous enzymes (QQ enzymes) or chemical analogs (QS inhibitors), which can be competitive/noncompetitive inhibitors of QS signals. Therefore, according to Grandclément et al. [3], "the term QQ encompasses a wide range of complex occurrences and mechanisms." Moreover, the efficient characterization of QS signaling molecules and their QQ counterparts have revealed that QS inhibitors are significantly more useful than traditional antimicrobials as they put less selection pressure on bacteria by not inducing cell death directly, thereby delaying the onset of antimicrobial resistance. Since time immemorial, many chemicals originating from plants, especially in the form of secondary metabolites, have been employed for their QS inhibiting capability. The antimicrobial activity of these plant-derived compounds is primarily attributed to phytoconstituents such as phenolic compounds, flavonoids, quinones, saponins, tannins, terpenoids, and alkaloids, whose functional and structural organizations are the cause of their QS inhibitory potential. There is a growing consensus that natural plant-derived compounds and their bioactive constituents are exceptionally potent, which can substitute conventional antibiotics. In a recent study, Niaouli essential oil (EO) and its major component 1,8-cineole have been found to be effective against *P. aeruginosa* PAO1 by competitively inhibiting QS [4]. *Lippia origanoides*, *Thymus* spp., and *Satureja hortensis* oil exhibited antibiofilm and QSI activities against human pathogenic bacteria [5, 6]. Furthermore, EOs and their bioactive compounds are eco-friendly and are not liable to bacterial resistance strategies [7]. Citral (a terpenoid), an integral constituent (30%–40%) of essential oil of lemongrass (EOL), is a potent antibacterial, antifungal, palliative, antiparasitic, as well as antianxiety and antidepressant compound whose applicability for curative purposes is rationalized by the fact that the continued vulnerability of its use has not confronted resistance among microorganisms [8, 9]. The full potential of phytoconstituents of EOL remains unexplored, despite their highly efficacious property of QSI at subinhibitory concentration. Researchers have previously shown that plant extracts and their bioactive components (phytochemicals) could efficiently hinder the intra- and interspecific communication system of the microbes, thereby blocking the pathway for microbial pathogenesis inside the host [10–12]. In this context, EO and their phytochemicals are considered to be safe for human use due to their low molecular mass and chemical stability [13].

The primary focus of the study is on quorum sensing inhibitory (QSI) potential of EO of citral and its polymer-based nanoparticle. Citral belongs to a terpenoid class of phytoconstituents, which is primarily attributed to the antibacterial property of EOL [14]. According to the U.S. Food and Drug Administration (FDA), citral is standardly acclaimed as safe (GRAS 182.10). It is an antibacterial chemical that has been shown to be effective against lethal Gram-positive and Gram-negative bacteria such as *Escherichia coli* strain O157:H7, *Salmonella typhimurium*, *Listeria monocytogenes*, and *Staphylococcus aureus* [15]. Existing literature supports the fact that its effectiveness against *P. aeruginosa* and associated antibacterial activity has yet to be fully demonstrated. Despite being an insoluble hydrophobic compound, citral is completely immiscible in inorganic solvents, incompatible with physiological system, and highly unstable at room temperature. Therefore, its applicability for both in vitro and in vivo purposes would be quite tedious [16, 17]. Encapsulation of citral in the form of nanoparticles, on the other hand, unveiled the much anticipated inhibition of the QS signaling molecules. Various encapsulation procedures have been studied including oil-in-water emulsion, multilayer emulsions, nanohydrogel, polymer encapsulation (such as cyclodextrin-inclusion complexes, polyacrylamide, and alginate polymerization), and self-assembly delivery systems [16–18]. Encapsulation of citral, thus, enhanced the functional potential and antimicrobial property of free oil, which has wide range of applicability from food industry to biomedical and agricultural sector.

Owing to the immense potential of citral, the anti-QS and antibiofilm effects of citral nanoparticles, as well as their characterization, were explored in this article. The secondary focus of the study lies on the insecticidal potential of the EOC. Due to the destruction caused by the insect pests, including fruit fly species against many economically important fruits, it is obligatory to search for alternative strategy in order to target major insect pests and associated microbes with these species. Insecticide resistance has increased as a result of the widespread usage of pesticides making the research focus shifting toward alternative pest management tools, so that potential risks to biodiversity, including nontarget organisms, could be reduced. Moreover, the drosophilids are the well-known carriers/vectors of pathogenic microbes leading to potential risk of infections among humans [19–21]; hence, effective management of these pests requires utmost attention. In the current study, the QSI activity of citral and its nanoparticle (polymer-based) against *P. aeruginosa* PAO1 have been investigated. Moreover, the toxic effect of citral against *Drosophila melanogaster* demonstrated insecticidal potential of citral, which can be further exploited against other pest species in India.

2. Materials and Methods

2.1. Maintenance of Bacterial Strains. Two biosensor strains, namely, *Agrobacterium tumefaciens* NLT4 and *E. coli* MG4

(both obtained from Jo Handelsman, University of Wisconsin, USA), were used in the present study, which were incubated at 28°C and 37°C, respectively, overnight under static conditions. Two laboratory isolates *E. coli* and *S. aureus* and standard strain of *P. aeruginosa* PAO1 (MTCC-3541, obtained from BH Iglweski, Department of Microbiology and Immunology, University of Rochester, USA) were cultured in Luria Broth (LB) at 37°C overnight (150 rpm).

2.2. Drosophila melanogaster Collection and Rearing. Wild caught Canton-S flies (*D. melanogaster*) were collected for experimental purpose from Kharar, Punjab (latitude and longitude coordinates: 30.751278 and 76.637192). Flies were grown under laboratory conditions (25 ± 1°C and 60%–70% relative humidity) by rearing on standard *Drosophila* medium, which consists of the predetermined fractions of various components such as agar–agar (15 g), dry yeast powder (40 g), sugar (64 g), and corn meal powder (72 g) per liter of water. Sodium benzoate (3 g) and propionic acid (6 ml) were also added as antimicrobial agents.

2.3. Estimation of Minimum Inhibitory Concentration (MIC) of Citral. Minimum inhibitory concentration (MIC) of citral required to inhibit the growth of *P. aeruginosa* PAO1 was evaluated by colorimetric method using resazurin microtiter assay (REMA) as described by Drummond and Waigh [22]. Briefly, stock solution of citral was serially diluted from 40% to 5% (in 10% dimethyl sulfoxide (DMSO)), followed by incubation at 37°C for 18 hr. After the addition of 10 μl of 0.01% resazurin dye (incubated for 1 hr), the maximum dilution showing no color change (from blue to pink) was considered as the MIC of citral.

2.4. Evaluation of Quorum Sensing Inhibitory (QSI) Activity of Citral. The estimation of QSI activity of citral was performed by the method of Shaw et al. [23] in which acyl homoserine lactone (AHL) was extracted by inoculating *P. aeruginosa* PAO1 in LB at 37°C (overnight) under continuous shaking conditions (150 rpm). The resulting culture was then centrifuged at 10,000 rpm for 15 min and the supernatant collected was pooled. AHL was extracted by centrifugation at 10,000 rpm for 15 min and the supernatant was dissolved in acidified ethyl acetate (0.01%) at 4°C (overnight). The organic layer was separated and the ethyl acetate was removed using Rotavapor resulting in 1 ml of AHL solution in the supernatant. The solution was stored at 4°C for further use. About 100 μl of extracted AHL was spread on a petri plate with initially streaked overnight culture of *A. tumefaciens* NLT4 and *E. coli* MG4 in separate plates. The petri plates were kept undisturbed at room temperature (RT) for 10 min. About 30 μl of citral (50%, 25%, 20%, and 15% in 5% DSMO) was loaded in 5 mm diameter wells punched on the plates. Negative control well contained 5% DMSO. Incubation at 28°C (*A. tumefaciens* streaked plates) and 30°C (*E. coli* MG4 streaked plates) for overnight was given and observed for degradation of AHL (colorless zones) on the next day.

2.5. Synthesis of Chitosan-Based Nanoparticles. Polymeric-based citral nanoparticles were synthesized by the method of Anitha et al. [24] in which chitosan sulfate (CS) and tripolyphosphate (TPP) (Sigma-Aldrich Chemical Co. Ltd., St. Louis, USA) were combined in different ratios (1 : 1, 1 : 2, 3 : 1 (CS:TPP) (v/v)). Briefly, citral (6% in methanol) was loaded to CS (1% acetic acid) solution dropwise followed by TPP (in high-performance liquid chromatography (HPLC) grade water) by continuous magnetic stirring for 1 hr. Residual methanol was evaporated using Rotavapor. Opalescent formulation was chosen for further experimentation.

2.5.1. Characterization of Nanoparticles. Citral nanoparticles were characterized by following parameters: particle size, zeta potential, polydispersity index (PDI), field-emission scanning electron microscopy (FE-SEM), entrapment efficiency (%EE), and in vitro release kinetics. Particle size and PDI were analyzed by Zetasizer Nano ZS (Malvern Instruments, UK) at 25°C [25]. Malvern Instruments Dispersion Technology software (version 4.0) was used to control and analyze all data from the instrument [26]. FE-SEM was performed using Joel Ion Sputter (JFC-1100) at Sophisticated Analytical Instrumentation Facility (SAIF), Panjab University, Chandigarh. The samples were examined by using FE-SEM model S-4160 (Hitachi, Japan). The %EE of citral within the CS-TPP nanoparticles and in vitro release profile was determined by the method of Sharma et al. [27]. The in vitro release profile of citral from nanoparticles was carried in order to understand the release behavior of citral from nanoparticles for sustained release of citral in vivo. The study was carried out at two different pH (5 and 7.4) using acetate buffer and phosphate-buffered saline (PBS), respectively, as release medium to mimic the in vivo conditions. The %EE was calculated using the following formula:

$$\%\text{EE} = \frac{\text{Total amount of loaded essential oils}}{\text{Initial amount of loaded essential oils}} \times 100. \quad (1)$$

2.6. Estimation of Minimum Inhibitory Concentration (MIC) of Citral Nanoparticles. MIC of citral nanoparticles was determined by the method of Jadhav et al. [28] with slight modifications. Briefly, citral nanoparticles (100, 90, 80, 70, 60, and 50 μl) were added to 5 ml of LB tubes separately, followed by 50 μl of OD (absorbance at 600 nm = 0.3) set culture of *P. aeruginosa* PAO1. Positive control tube contained only 50 μl OD set culture, while negative control tube contained uninoculated media. After overnight incubation at 37°C under shaking conditions, tubes were then observed for visible growth. The results were interpreted as the maximum dilution, which showed that no visible growth in tubes was chosen as MIC of citral nanoparticles. The experiment was performed in triplicates.

2.7. Estimation of Sub-Minimum Inhibitory Concentration (Sub-MIC) of Citral Nanoparticles. Sub-MIC was determined using growth curve analysis to measure a concentration at which the citral nanoparticles could attenuate the virulence of *P. aeruginosa* without killing it. Briefly, citral nanoparticles (100, 90, 80, 70, 60 μl/ml) were added to 20 ml of LB. 200 μl

of OD 600 set culture (0.3–0.4) of *P. aeruginosa* PAO1 was added to each tube. A blank flask contained the respective volume of bare nanoparticles, while a positive control flask contained 200 μl of culture only. Incubation at 37°C under shaking conditions (150 rpm) was given and an aliquot was withdrawn at different time intervals: 0, 2, 4, 6, 8, 10, 12, and 24 hr for measuring the absorbance at 595 nm. The blank absorbance value was subtracted from the respective absorbance values of flasks containing citral nanoparticles. Growth curve (OD (at 595 nm) vs. time (in hours)) was plotted using Microsoft Excel. The sub-MIC was chosen as that concentration of citral nanoparticles when it does not have an effect on growth of *P. aeruginosa*.

2.8. Qualitative Estimation of QSI Activity of Citral Nanoparticles. QSI activity of citral nanoparticles and citral (alone) was performed using agar well diffusion assay. AHL was extracted from *P. aeruginosa* PAO1 as described earlier. Wells were loaded with 30 μl of citral, citral nanoparticles (90, 80, 70, 60 μl/ml), and bare nanoparticles. The plates were incubated at 28°C overnight and observed for degradation of AHL (colorless zones) on the next day. The inhibition zones around the wells corresponded to the bactericidal activity, while the colorless zones of colonies represented the anti-QS potential of the agent.

2.9. Evaluation of Antibiofilm Activity of Citral Nanoparticles

2.9.1. Biofilm Inhibition Assay. Biofilm formation and the inhibition effect due to citral nanoparticles were performed according to the method of Stepanović et al. [29]. Briefly, 100 μl of overnight grown *P. aeruginosa* PAO1 was added to each well of 96-well microtiter plate. Negative control well contained 200 μl of LB, while the treatment wells contained citral nanoparticles (90, 80, 70, 60 μl/ml) and citral (2 μl/ml), separately along with 100 μl of LB to equilibrate the volume. To allow biofilm formation, incubation at 37°C (overnight) under static conditions was given and after 18–24 hr, spent media was replaced by fresh media (to eliminate planktonic cells) by washing thrice with 0.1 M sterile PBS (pH 7.2). The inner surface of the wells was scrapped using a sterile scalpel blade, and then, the cells were suspended in 100 μl of PBS (pH 7.2). Everyday, the suspended cells in PBS were serially diluted and 25 μl of each dilution was plated on MacConkey agar plates (incubation at 37°C for 18 hr). The log bacterial count (log10 colony-forming unit (CFU)/ml) was determined consecutively for 7 days.

2.9.2. Microscopic Analysis (FE-SEM). Microscopic visualization of treated and untreated biofilm cells was done using FE-SEM. Treated biofilm cells were formed in the presence of sub-MIC of citral nanoparticles and citral over acid-itched coverslips for 48 hr. Coverslips were then fixed using 2.5% glutaraldehyde in 0.1 mM PBS for 6–12 hr at 22°C, followed by washing with 0.1 M sterile PBS (pH 7.2) and dehydration with increasing concentrations of ethanol (50%–100%) at RT. Samples analysis was done using Joel Ion Sputter (JFC-1100) at SAIF, Panjab University, Chandigarh.

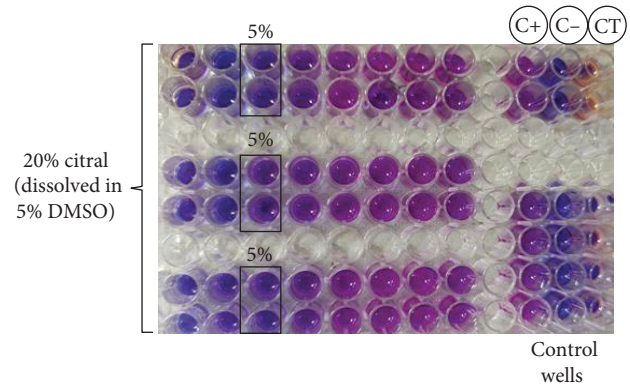

FIGURE 1: A 96-well microtiter plate showing MIC of citral against *P. aeruginosa* PAO1. (C+): positive control well; (C–): negative control well; (CT): citral control well.

2.10. Insecticidal Activity of Citral against Drosophila melanogaster. Insecticidal potential of citral was determined against *D. melanogaster* for the following citral concentrations: 0.5%, 0.2%, 1%, 3%, and 5%. Briefly, 20 females and 20 males (6 days old) of *D. melanogaster* were kept on standard *Drosophila* culture medium for 6–8 hr of egg laying. Around 30 eggs were counted and placed in each petri plate containing varying concentrations of citral, followed by incubation into a biochemical oxygen demand incubator at 25°C. The assay measured following attributes: %adult emergence, %survivability, and development time. Negative control consisted of 0.1% Tween 80 supplemented in *Drosophila* culture medium without citral.

2.11. Statistical Analysis. Microsoft Excel 2010 was used for statistical analysis of the data. The experiments were performed in triplicates, which were represented as the average of standard deviation. Tests performed were Student's *t*-test, one-way and two-way ANOVA, which analyzed the differences between control and test treatments. Data with p-value < 0.05 were considered statistically significant.

3. Results and Discussion

3.1. Minimum Inhibitory Concentration of Citral. MIC of citral was determined by resazurin dye reduction assay in which color change using resazurin dye (from blue to pink) is the indicator of cell viability. Citral (20% v/v in 5% DMSO) was serially diluted in 96-well microtiter plates. Negative control well consisted of media without inoculum (no viable cells), while the positive control well consisted of culture media (indicator of viable bacterial cells). MIC of citral required to inhibit *P. aeruginosa* growth was around 5% (v/v), as determined by the assay (Figure 1). The results were concurrent with previous findings of Hayes and Markovic [30], Aiemsaard et al. [31], and Adukwu et al. [14], where it was claimed that citral is effective in inhibiting the growth of pathogenic bacteria of clinical significance. According to Gill et al. [32], antibacterial potential of EO could be primarily due to the individual components of the oil, acting synergistically for more potent effect.

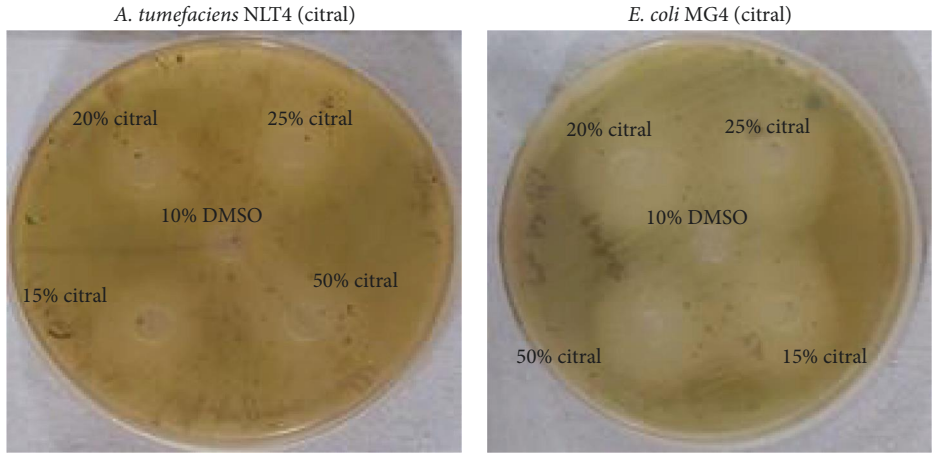

Figure 2: Plates showing QSI activity of citral against: (a) *A. tumefaciens* NLT4; (b) *E. coli* MG4.

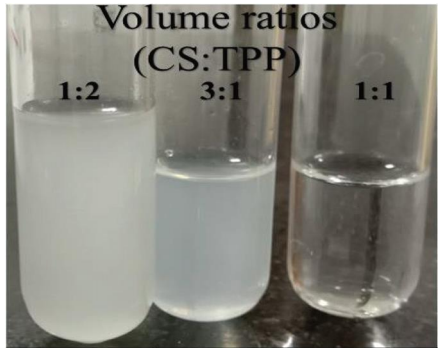

Figure 3: Chitosan-tripolyphosphate (CS-TPP)-based citral nanoparticles.

3.2. Quorum-Sensing Inhibitory (QSI) Activity of Citral. QSI activity of citral was determined using biosensor strains: *A. tumefaciens* NLT4 and *E. coli* MG4; the nonpigmented colonies around the wells are the indicator of QSI activity, while complete inhibition of growth represented the antibacterial activity of citral. These colorless colonies formed around the wells qualitatively represented the attenuation of virulence or QS potential of the citral. Control well contained 10% DMSO in sterile distilled water. As shown in Figure 2, all concentrations of citral exhibited antibacterial and QSI activity but at 20% and 25%, prominent anti-QS activity can be clearly observed. At 20% and 25% of pure citral, colorless colonies were formed at vicinity of inhibitory zone around the well. In contrast, 15% of citral showed weak antibacterial activity, while 50% of oil showed clear inhibitory zone around the well.

3.3. Synthesis of Citral Nanoparticles. CS- and TPP-based citral nanoparticles were prepared for the encapsulation of oil in order to curb the problem of solubility and delivery of EO of citral. As shown in Figure 3, volume ratio of 1 : 2 (CS:TPP) formed opalescent formulation without the aggregate formation. Hence, this volume ratio was used for further experiments. Loading of citral in the form of polymeric nanoparticles showed that citral completely got soluble when emulsified in CS-TPP nanoparticle formulation. This formulation combated the problem for delivery of citral for in vivo applications.

3.3.1. Characterization of Citral Nanoparticles. Characterization of citral nanoparticles was done by Zetasizer where average hydrodyanamic size and PDI were found to be 209 ± 22.4 nm and 0.490, respectively, as shown in Figure 4(a). These results verified that citral nanoparticles were relatively uniform or homogeneously distributed within the colloidal system in accordance with the particle size. The results of zeta potential (surface charge indicator), as shown in Figure 4(b), elucidated that the potential difference between the nanoparticle and its dispersion medium was 20.9 ± 3.54 mV. Both zeta potential and PDI are the parameters of stable nanoformulation formation. Moreover, FE-SEM analysis was performed to visualize the topological details (size and shape) of formed citral nanoparticles, which displayed typically spherical shape of nanoparticles, as shown in Figure 4(c). While the shape of nanoparticle could influence its delivery have been the topic of research among the scholars, the significance of a particular shape of nanomaterial is still to be delineated. Hence, a particular shape of nanosized materials can indispensably affect its transportation and absorption within the human body, regardless of the specific routes of administration. A study done by Chenthamara et al. [33] claimed that, "the spherical nanoparticles transverse freely due to their basic symmetry, while the nonspherical particles thrust or sink within the dispersion medium." The in vitro release profile revealed that there was an initial fast release till the first 6 hr where citral was released up to 46% in pH 5 (sodium acetate buffer) and 38% in pH 7.4 (PBS). The release rate slowed down after 24 hr, but sustained release was observed till 144 hr. Drug release was up to 80% and 78% at pH 5 and

Results

		Size (d.nm)	%intensity	Standard deviation (d.nm)
Z-average (d.nm) 209.9	Peak 1	421.2	95.1	329.8
PDI 0.490	Peak 2	37.06	4.9	8.490
Intercept 0.881	Peak 3	0.000	0.0	0.000
Result quality Good				

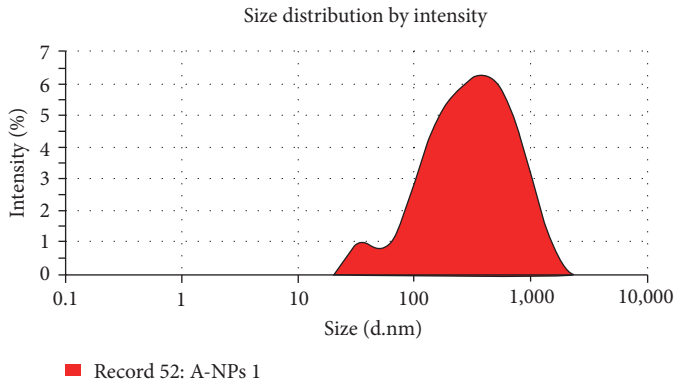

(a)

Results

		Mean (mV)	Area (%)	Standard deviation
Zeta potential (mV) 20.9	Peak 1	20.9	100.0	3.54
Zeta deviation (mV) 3.54	Peak 2	0.00	0.0	0.00
Conductivity (mS/cm) 0.836	Peak 3	0.00	0.0	0.00
Result quality Good				

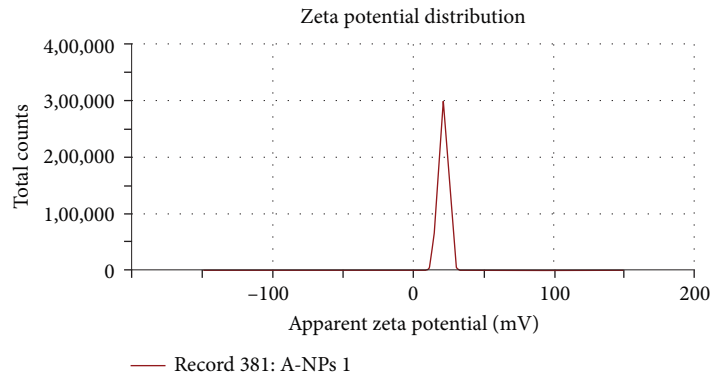

(b)

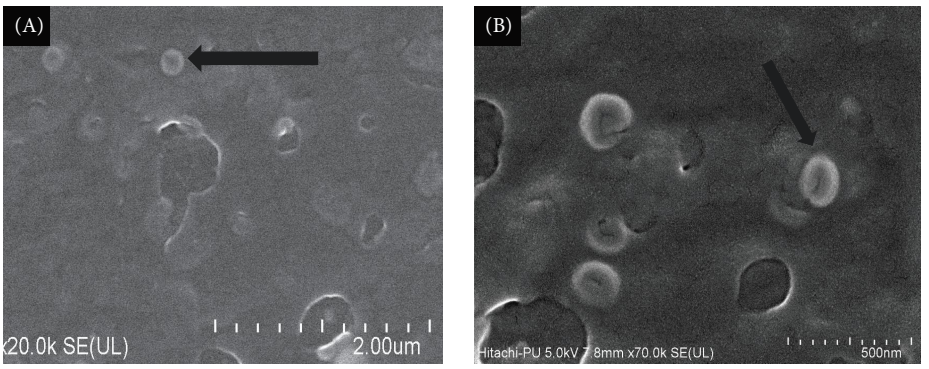

(A) Citral-loaded chitosan nanoparticles (B) Citral-loaded chitosan nanoparticles

(c)

Figure 4: Continued.

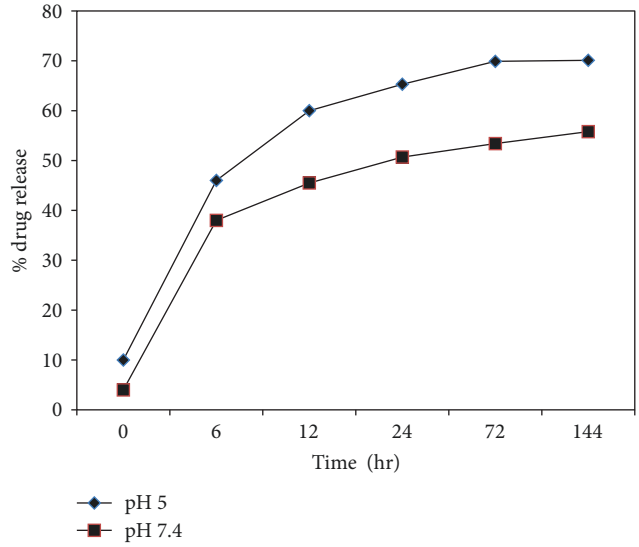

(d)

Figure 4: (a) Data sheet representing the *z*-average (particle size), polydispersity index (PDI), and quality check of citral nanoparticles. (b) Data sheet representing zeta potential (mV) and result quality of citral nanoparticles. (c) (A and B) FE-SEM images of citral nanoparticles. Arrows in the image denote formed nanoparticles. (d) In vitro release profile of citral from nanoparticles at neutral (7.4) and acidic (5) pH.

pH 7.4, respectively (Figure 4(d)). These results were concurrent with previous study, which indicated a time- and pH-dependent in vitro release of EOL into release media with a rapid initial release of EO and a steady state phase of EO at the later stages [34]. The %EE of citral oil was found to be around 52.56% ± 4.89%. These results are similar to those in the former investigation, except for results of microencapsulation efficiency of lemongrass oil using spray drying where %EE was 84.75% [35]. However, %EE of lemongrass oil encapsulated in CS nanoparticles was 44.82% ±2.80% as investigated by Negi and Kesari [36].

3.4. Minimum Inhibitory Concentration (MIC) of Citral Nanoparticles. For the estimation of MIC, macrodilution tube method was performed in order to elucidate the minimum concentration of citral nanoparticles required to inhibit the growth of *P. aeruginosa* PAO1. Estimated MIC of citral nanoparticles was observed to be 100 μl/ml relative to the negative control with no visible growth. as shown in Figure 5.

3.5. Sub-MIC of Citral Nanoparticles. In order to determine the subinhibitory concentration of citral nanoparticles, growth profile of standard strain of *P. aeruginosa* was created by growing the bacterium in the presence and absence of citral nanoparticles below the MIC. According to the definition, sub-MIC is that concentration of the drug/agent at which virulence or pathogenicity of the strain is suppressed instead of doses, which can directly kill the microorganism. Growth profile of *P. aeruginosa* observed over a period of 10 hr demonstrated that the lag phase (initial hours from 0 to 2 hr) showed no significant alteration in the growth of *P. aeruginosa*. However, during exponential phase (4–10 hr), a relatively similar growth profile was observed with citral nanoparticles at 80 μl/ml and the control (without treatment). Hence, growth kinetics showed that this volume of citral

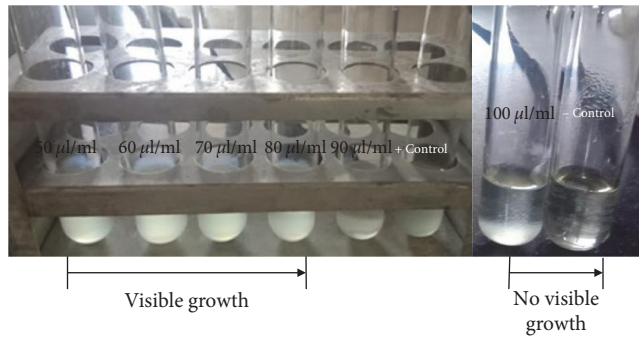

Figure 5: Macrodilution tube method representing MIC of citral nanoparticles. −Control: negative control tube (only LB); +control: positive control tube (culture media without treatment).

nanoparticles did not significantly inhibit the growth of *P. aeruginosa* and this value was further deployed in vitro experiments of QSI activity. In contrast, a considerable inhibition of growth was observed at 100 and 90 μl/ml of citral nanoparticle, as shown in Figure 6.

3.6. QSI Activity of Citral Nanoparticles. Biosensor strain, *A. tumefaciens* NLT4, was used to determine the potential of citral nanoparticles to inhibit long-chain AHLs in a concentration-dependent manner. A colorless zone of colonies around the wells was observed at sub-MIC (80 μl) and below MIC (60, 70, 90 μl/ml) of citral nanoparticles, which clearly indicated the QSI activity. Antibacterial activity was more evident at higher concentration (90 μl/ml) of citral nanoparticles than QSI activity, as shown in Figures 7(a) and 7(b), whereas lower concentrations (60 and 70 μl/ml) showed minimal to no QSI activity, as shown in Figure 7(c). Moreover, encapsulated citral showed better QSI activity than citral alone. This is the first data reporting the QSI

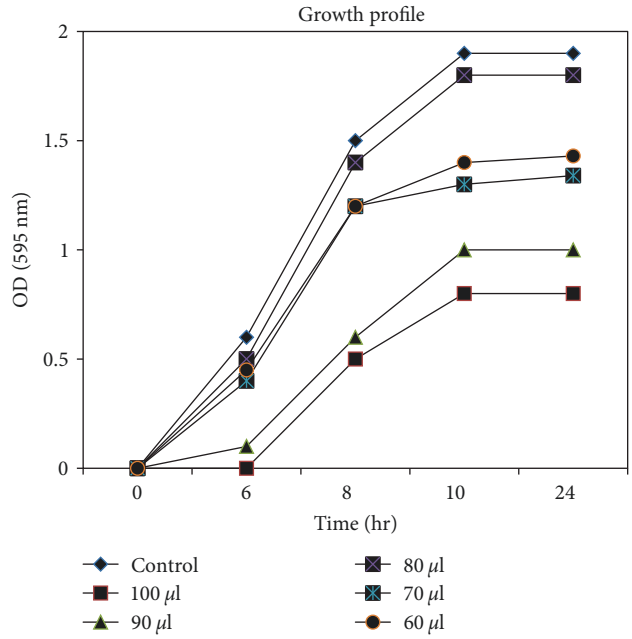

Figure 6: Growth kinetics of *P. aeruginosa* PAO1 with and without citral nanoparticle treatment.

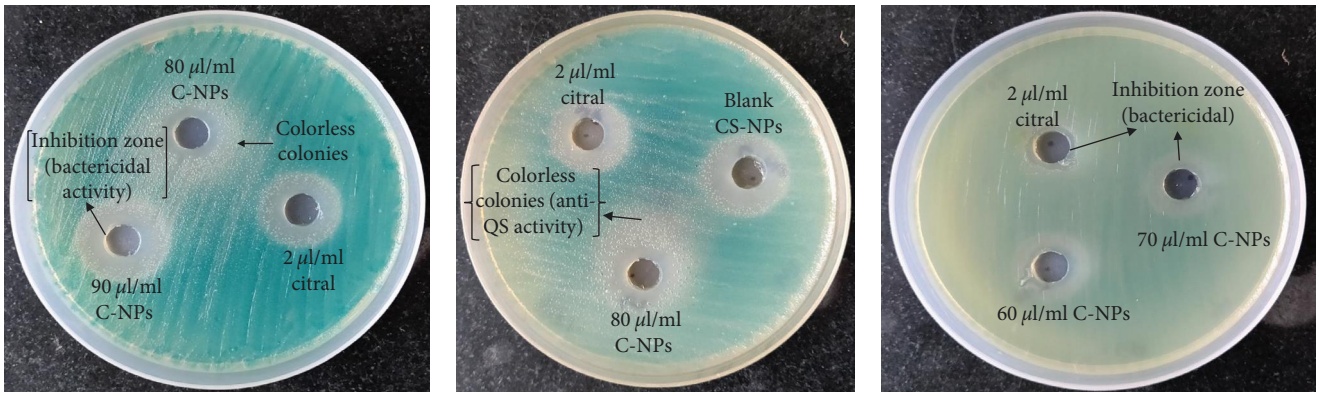

(a) (b) (c)

Figure 7: Quorum sensing inhibitory (QSI) activities of (a) 80 μl/ml of citral nanoparticles (C–NPs) and 90 μl/ml of citral nanoparticles, (b) blank chitosan nanoparticles (CS–NPs) and 80 μl/ml nanoparticles, and (c) 60 and 70 μl/ml of citral nanoparticles, compared with citral alone.

activity of citral nanoparticles, which can be further used for biomedical appications.

From the results of above experiments, it can be concluded that the antimicrobial and QSI effects of citral nanoparticles are more potent than the free form of citral. These findings are coherent with similar study with cinnamon (*Cinnamomum zeylanicum*), thyme (*Thymus vulgaris*), clove (*Syzygium aromaticum*), and *Schinus molle* EO when encapsulated with the CS nanoparticles and showed enhanced antimicrobial activity than the CS and EOs alone [37–39]. However, not a single article reports QSI activity of nanoparticles/EOs in comparison with their free EO. The results support the fact that the nanoparticles could prove to be an effective agent in controlling lethal microbial infections, possibly due to the synergistic effect of CS-TPP-based nanoparticles. However, there are various drawbacks and implications associated with the construction of suitable drug delivery systems such as carrier for the targeted drug delivery and physical and chemical factors, which are pivotal for the bioavailability of drug and could offer potential pathway to combat several identified target diseases.

3.7. Effect of Citral Nanoparticles on Biofilm Phenotypes. The effect of citral nanoparticles was phenotypically observed on biofilm-forming ability of *P. aeruginosa* for up to 7 days. The results (Figure 8(a)) clearly depicted that biofilm-forming capacity of the bacterium retarded in the presence of citral nanoparticles at all concentrations. However, at sub-MIC, significant inhibition of about 3.2 log and 2.0 log was observed on 6th and 7th days (p-value < 0.05) in comparison with the untreated control. Relative to citral alone-treated biofilm cells, at a very low concentration of 80 μl/ml, citral nanoparticles showed antibiofilm activity, which is quite suitable for in vivo purposes with no to less toxicity for clinical patients.

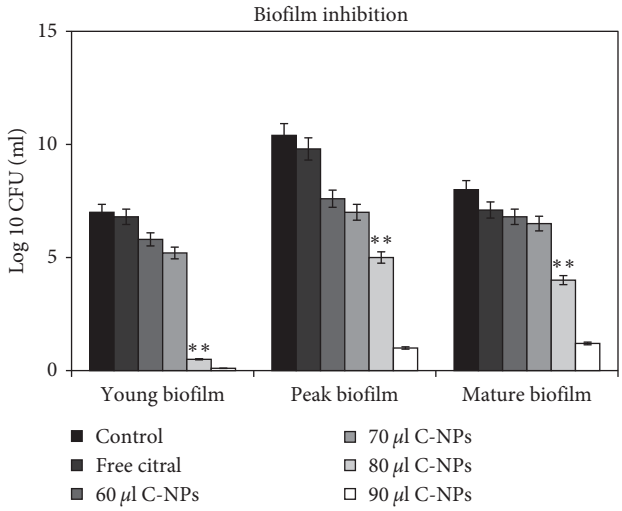

(a)

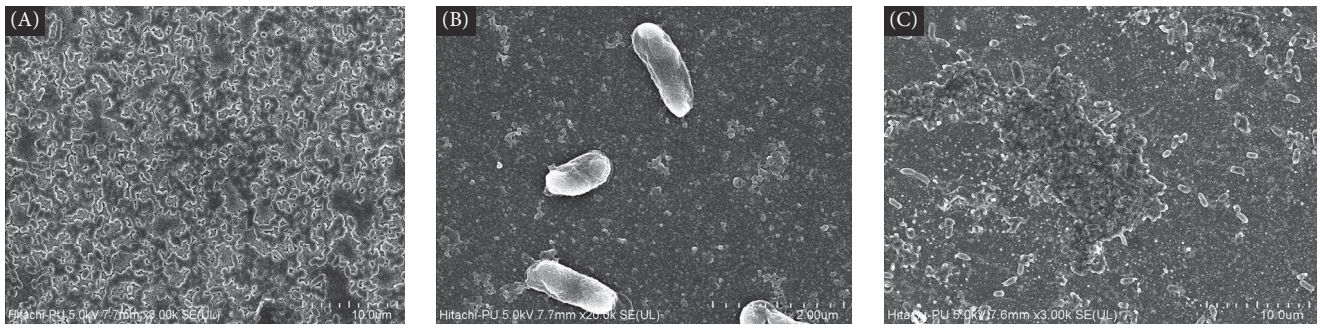

(A) Control biofilm cells (B) Intact biofilm cells (C) Citral (alone)-treated cells

(D) Loss of cell integrity (E) Citral-loaded nanoparticles-treated cells (F) Citral-loaded nanoparticles-treated cells

(b)

Figure 8: (a) Bacterial load of biofilm cells grown for 7 days treated with citral nanoparticles and citral (alone). (b) FE-SEM analysis of: (A and B) control biofilm cells; (C and D) citral (2 μl/ml) alone; (E and F) citral nanoparticles (80 μl/ml) treated biofilm cells.

Antibiofilm effect of citral nanoparticles was also confirmed by FE-SEM analysis. 48 hr biofilm cells of *P. aeruginosa* were grown in the absence (control) and presence of sub-MIC of citral nanoparticles over acid-itched coverslips under static conditions. The treated cells showed a drastic reduction in biofilm thickness. The entire structure of biofilm cells (amorphous) was skewed when treated with at sub-MIC of citral nanoparticles relative to citral treatment, where insignificant deformation was observed, as shown in Figures 8(B) and 8(D). Thus, FE-SEM analysis of biofilms validated the fact that the citral nanoparticles (Figure 8(B)–8(D)) are efficient in imparting cell distortion and impaired architecture to biofilm cells at subinhibitory conditions.

3.8. Toxic Effect of Essential Oil of Citral at Different Concentrations against Drosophila melanogaster. Insecticidal potential of EO of citral was also monitored against *D. melanogaster* in terms of elongation in developmental

Table 1: Toxic effect of essential oil of citral at different concentrations on the developmental stages of *Drosophila melanogaster*.

Treatments (%)	Development time (average)		Adult hatchability (%)	Survivability (%)
	Third instar larvae (days)	Pupa (hr)		
0 (negative control)	4	48	81.4	44
0.2	6	50	78.9	30
0.5	6	39	78.9	34
1	5.5	49	76.1	36
3	11	72	Unfinished	0
5	Unfinished	Unfinished	Unfinished	0

period, % adult hatchability, and % survivability of egg. All obtained results are summarized in Table 1.

4. Conclusion

Results of the present study elucidated that citral nanoparticles could effectively suppress the pathogenicity of *P. aeruginosa* and as a result, it can be utilized for the targeted delivery of citral to treat lethal infections. This property of citral nanoparticles can be used for drug targeting, which can be exploited in treating bacterial complications in clinical settings, including *P. aeruginosa*. Moreover, the elucidation of insecticidal activity of citral against *D. melanogaster* could further be exploited in controlling pests of agricultural importance and associated opportunistic microbes with these pest species of fruit fly. The results of the present study clearly depicted that encapsulation of citral in the form of nanoparticles enhanced the potential of citral in targeted delivery of drug in vivo and, hence, could be used as a potent substitute to conventional antibiotics and chemical insecticides, combating the major problem of antibiotic and insecticide resistance in nature.

Data Availability

The data used to support the findings of this study are included within the article. Further data or information is available from the corresponding author upon request.

Conflicts of Interest

The authors declare that they have no conflicts of interest.

Funding

This work was supported by Panjab University, Sector 14, Chandigarh, and Chandigarh University, Gharuan, Punjab, India.

References

[1] M. F. Moradali, S. Ghods, and B. H. A. Rehm, "*Pseudomonas aeruginosa* lifestyle: a paradigm for adaptation, survival, and persistence," *Frontiers in Cellular and Infection Microbiology*, vol. 7, Article ID 39, 2017.

[2] A. Tahrioui, R. Duchesne, E. Bouffartigues et al., "Extracellular DNA release, quorum sensing, and PrrF1/F2 small RNAs are key players in *Pseudomonas aeruginosa* tobramycin-enhanced biofilm formation," *npj Biofilms and Microbiomes*, vol. 5, no. 1, Article ID 15, 2019.

[3] C. Grandclément, M. Tannières, S. Moréra, Y. Dessaux, and D. Faure, "Quorum quenching: role in nature and applied developments," *FEMS Microbiology Reviews*, vol. 40, no. 1, pp. 86–116, 2016.

[4] E. Onem, A. Soyocak, M. T. Muhammed, and A. Ak, "In vitro and in silico assessment of the potential of niaouli essential oil as a quorum sensing inhibitor of biofilm formation and its effects on fibroblast cell viability," *Brazilian Archives of Biology and Technology*, vol. 64, Article ID e21200782, 2021.

[5] M. Cáceres, W. Hidalgo, E. Stashenko, R. Torres, and C. Ortiz, "Essential oils of aromatic plants with antibacterial, anti-biofilm and anti-quorum sensing activities against pathogenic bacteria," *Antibiotics*, vol. 9, no. 4, Article ID 147, 2020.

[6] A. Sharifi, A. Mohammadzadeh, T. Zahraei Salehi, and P. Mahmoodi, "Antibacterial, antibiofilm and antiquorum sensing effects of *Thymus daenensis* and *Satureja hortensis* essential oils against *Staphylococcus aureus* isolates," *Journal of Applied Microbiology*, vol. 124, no. 2, pp. 379–388, 2018.

[7] A. Borges, A. C. Abreu, C. Dias, M. J. Saavedra, F. Borges, and M. Simões, "New perspectives on the use of phytochemicals as an emergent strategy to control bacterial infections including biofilms," *Molecules*, vol. 21, no. 7, Article ID 877, 2016.

[8] P. Hersch-Martínez, B. E. Leaños-Miranda, and F. Solórzano-Santos, "Antibacterial effects of commercial essential oils over locally prevalent pathogenic strains in Mexico," *Fitoterapia*, vol. 76, no. 5, pp. 453–457, 2005.

[9] H. B. Martins, N. das Neves Selis, C. L. Silva e Souza et al., "Anti-inflammatory activity of the essential oil citral in experimental infection with *Staphylococcus aureus* in a model air pouch," *Evidence-Based Complementary and Alternative Medicine*, vol. 2017, Article ID 2505610, 10 pages, 2017.

[10] D. A. Vattem, K. Mihalik, S. H. Crixell, and R. J. C. McLean, "Dietary phytochemicals as quorum sensing inhibitors," *Fitoterapia*, vol. 78, no. 4, pp. 302–310, 2007.

[11] A. J. Bai and R. R. Vittal, "Quorum sensing inhibitory and anti-biofilm activity of essential oils and their *in vivo* efficacy in food systems," *Food Biotechnology*, vol. 28, no. 3, pp. 269–292, 2014.

[12] R. Barbieri, E. Coppo, A. Marchese et al., "Phytochemicals for human disease: an update on plant-derived compounds antibacterial activity," *Microbiological Research*, vol. 196, pp. 44–68, 2017.

[13] H. Tang, G. Porras, M. M. Brown et al., "Triterpenoid acids isolated from *Schinus terebinthifolia* fruits reduce *Staphylococcus aureus* virulence and abate dermonecrosis," *Scientific Reports*, vol. 10, no. 1, Article ID 8046, 2020.

[14] E. C. Adukwu, S. C. H. Allen, and C. A. Phillips, "The antibiofilm activity of lemongrass (*Cymbopogon flexuosus*) and grapefruit (*Citrus paradisi*) essential oils against five strains of *Staphylococcus* aureus," *Journal of Applied Microbiology*, vol. 113, no. 5, pp. 1217–1227, 2012.

[15] C. Shi, K. Song, X. Zhang et al., "Antimicrobial activity and possible mechanism of action of citral against *Cronobacter sakazakii*," *PLOS ONE*, vol. 11, no. 7, Article ID e0159006, 2016.

[16] R. Peng, C. Du, A. Hu et al., "Fabrication of core-shell type poly(NIPAm)-encapsulated citral and its application on bamboo as an anti-molding coating," *RSC Advances*, vol. 11, no. 58, pp. 36884–36894, 2021.

[17] M. Maswal and A. A. Dar, "Formulation challenges in encapsulation and delivery of citral for improved food quality," *Food Hydrocolloids*, vol. 37, pp. 182–195, 2014.

[18] Z. Aytac, A. Celebioglu, Z. I. Yildiz, and T. Uyar, "Efficient encapsulation of citral in fast-dissolving polymer-free electrospun nanofibers of cyclodextrin inclusion complexes: high thermal stability, longer shelf-life, and enhanced water solubility of citral," *Nanomaterials*, vol. 8, no. 10, Article ID 793, 2018.

[19] C. Barreiro, H. Albano, J. Silva, and P. Teixeira, "Role of flies as vectors of foodborne pathogens in rural areas," *International Scholarly Research Notices*, vol. 2013, Article ID 718780, 7 pages, 2013.

[20] L. A. Ramírez-Camejo, G. Maldonado-Morales, and P. Bayman, "Differential microbial diversity in *Drosophila melanogaster*: are fruit flies potential vectors of opportunistic pathogens?" *International Journal of Microbiology*, vol. 2017, Article ID 8526385, 6 pages, 2017.

[21] E. P. Black, G. J. Hinrichs, S. J. Barcay, and D. B. Gardner, "Fruit flies as potential vectors of foodborne illness," *Journal of Food Protection*, vol. 81, no. 3, pp. 509–514, 2018.

[22] A. J. Drummond and R. D. Waigh, "The development of microbiological methods for phytochemical screening," *Recent Research Developments in Phytochemistry*, vol. 4, pp. 143–152, 2000.

[23] P. D. Shaw, G. Ping, S. L. Daly et al., "Detecting and characterizing *N*-acyl-homoserine lactone signal molecules by thin-layer chromatography," *Proceedings of the National Academy of Sciences*, vol. 94, no. 12, pp. 6034–6041, 1997.

[24] A. Anitha, V. G. Deepagan, V. V. Divya Rani, D. Menon, S. V. Nair, and R. Jayakumar, "Preparation, characterization, *in vitro* drug release and biological studies of curcumin loaded dextran sulphate-chitosan nanoparticles," *Carbohydrate Polymers*, vol. 84, no. 3, pp. 1158–1164, 2011.

[25] P.-J. Lu, W.-E. Fu, S.-C. Huang et al., "Methodology for sample preparation and size measurement of commercial ZnO nanoparticles," *Journal of Food and Drug Analysis*, vol. 26, no. 2, pp. 628–636, 2018.

[26] R. Tantra, P. Schulze, and P. Quincey, "Effect of nanoparticle concentration on zeta-potential measurement results and reproducibility," *Particuology*, vol. 8, no. 3, pp. 279–285, 2010.

[27] K. Sharma, P. Nirbhavane, S. Chhibber, and K. Harjai, "Sustained release of zingerone from polymeric nanoparticles: an anti-virulence strategy against *Pseudomonas aeruginosa*," *Journal of Bioactive and Compatible Polymers*, vol. 35, no. 6, pp. 538–553, 2020.

[28] S. Jadhav, R. Shah, M. Bhave, and E. A. Palombo, "Inhibitory activity of yarrow essential oil on *Listeria* planktonic cells and biofilms," *Food Control*, vol. 29, no. 1, pp. 125–130, 2013.

[29] S. Stepanović, D. Vuković, V. Hola et al., "Quantification of biofilm in microtiter plates: overview of testing conditions and practical recommendations for assessment of biofilm production by staphylococci," *Journal of Pathology, Microbiology and Immunology - the APMIS Journal*, vol. 115, no. 8, pp. 891–899, 2007.

[30] A. J. Hayes and B. Markovic, "Toxicity of Australian essential oil *Backhousia citriodora* (lemon myrtle). Part 1. Antimicrobial activity and in vitro cytotoxicity," *Food and Chemical Toxicology*, vol. 40, no. 4, pp. 535–543, 2002.

[31] J. Aiemsaard, S. Aiumlamai, C. Aromdee, S. Taweechaisupapong, and W. Khunkitti, "The effect of lemongrass oil and its major components on clinical isolate mastitis pathogens and their mechanisms of action on *Staphylococcus aureus* DMST 4745," *Research in Veterinary Science*, vol. 91, no. 3, pp. e31–e37, 2011.

[32] A. O. Gill, P. Delaquis, P. Russo, and R. A. Holley, "Evaluation of antilisterial action of cilantro oil on vacuum packed ham," *International Journal of Food Microbiology*, vol. 73, no. 1, pp. 83–92, 2002.

[33] D. Chenthamara, S. Subramaniam, S. G. Ramakrishnan et al., "Therapeutic efficacy of nanoparticles and routes of administration," *Biomaterials Research*, vol. 23, no. 1, Article ID 20, 2019.

[34] M. Soltanzadeh, S. H. Peighambardoust, B. Ghanbarzadeh, M. Mohammadi, and J. M. Lorenzo, "Chitosan nanoparticles encapsulating lemongrass (*Cymbopogon commutatus*) essential oil: physicochemical, structural, antimicrobial and in-vitro release properties," *International Journal of Biological Macromolecules*, vol. 192, pp. 1084–1097, 2021.

[35] N. P. Thuong Nhan, V. T. Thanh, M. H. Cang et al., "Microencapsulation of lemongrass (*Cymbopogon citratus*) essential oil via spray drying: effects of feed emulsion parameters," *Processes*, vol. 8, no. 1, Article ID 40, 2020.

[36] A. Negi and K. K. Kesari, "Chitosan nanoparticle encapsulation of antibacterial essential oils," *Micromachines*, vol. 13, no. 8, Article ID 1265, 2022.

[37] D. G. Barrera-Ruiz, G. C. Cuestas-Rosas, R. I. Sánchez-Mariñez et al., "Antibacterial activity of essential oils encapsulated in chitosan nanoparticles," *Food Science and Technology*, vol. 40, no. suppl 2, pp. 568–573, 2020.

[38] A. G. Luque-Alcaraz, M. O. Cortez-Rocha, C. A. Velázquez-Contreras et al., "Enhanced antifungal effect of chitosan/pepper tree (*Schinus molle*) essential oil bionanocomposites on the viability of *Aspergillus parasiticus* spores," *Journal of Nanomaterials*, vol. 2016, Article ID 6060137, 10 pages, 2016.

[39] M. Hadidi, S. Pouramin, F. Adinepour, S. Haghani, and S. M. Jafari, "Chitosan nanoparticles loaded with clove essential oil: characterization, antioxidant and antibacterial activities," *Carbohydrate Polymers*, vol. 236, Article ID 116075, 2020.

Hindawi
Journal of Nanomaterials
Volume 2022, Article ID 7238602, 16 pages
https://doi.org/10.1155/2022/7238602

Review Article

Recent Advances in Methods for Synthesis of Carbon Nanotubes and Carbon Nanocomposite and their Emerging Applications: A Descriptive Review

Amel Gacem,[1] **Shreya Modi**,[2] **Virendra Kumar Yadav**,[3] **Saiful Islam**,[4] **Aradhna Patel**,[5] **Vinars Dawane**,[6] **Mohammed Jameel**,[4] **Gajendra Kumar Inwati**,[7] **Satish Piplode**,[8] **Vijendra Singh Solanki**,[9] **and Anup Basnet**[10]

[1]*Department of Physics, Faculty of Sciences, University 20 Août 1955, Skikda, Algeria*
[2]*Department of Microbiology, Shri Sarvajanik Science College, Mehsana, Gujarat 384001, India*
[3]*Department of Biosciences, School of Liberal Arts & Sciences, Mody University of Science and Technology, Sikar, Rajasthan 332311, India*
[4]*Civil Engineering Department, College of Engineering, King Khalid University, Abha 61421, Saudi Arabia*
[5]*Department of Microbiology, Faculty of Sciences, Sankalchand Patel University, Mehsana, Gujarat 384315, India*
[6]*Department of Microbiology and Biotechnology, Sardar Vallabh Bhai Patel College, Mandleshwar, 451221, Madhya Pradesh, India*
[7]*Department of Chemistry, Medicaps University, Indore, Madhya Pradesh, 453331, India*
[8]*Department of Chemistry, SBS Govt. PG College, Hoshangabad Madhya Pradesh, 461775, Pipariya, India*
[9]*Department of Chemistry, School of Liberal Arts & Sciences, Mody University of Science and Technology, Sikar, Rajasthan 332311, India*
[10]*Department of Microbiology, Saint Xavier's College, Maitighar, Kathmandu 695586, Nepal*

Correspondence should be addressed to Anup Basnet; basnet.a@sxc.edu.np

Received 20 June 2022; Accepted 16 September 2022; Published 29 September 2022

Academic Editor: Seema Ramniwas

Nanomaterials have gained huge applications ever since their discoveries, especially in the field of electronics, medicine, research, and environmental cleanup. Nanomaterials have a high surface area-to-volume ratio along with high surface energies making them suitable for such wide applications. Carbon nanotubes (CNTs) and carbon nanocomposite (CNC) materials are remarkable nanomaterials that have become the backbone of most industries these days. Both materials have gained huge attention in the last decade by the scientific community. CNTs come in two variants, i.e., single-walled CNTs (SW-CNTS) and multiwalled CNTs (MW-CNTs). Due to their wider applications, CNT synthesis is currently emerging with the advancement in technology. Currently, CNTs are being synthesized by chemical as well as physical approaches. The current review article focuses on the vital research and application for the synthesis of CNTs depending on the quality of the nanotube materials. Controlled routes to their organization and assembly are also discussed in detail over here. The aim is to provide recent advances in the synthesis methods, of CNTs, their current applications, future applications, and the potential of agrowaste and industrial waste for the synthesis of CNTs and nanomaterials.

1. Introduction

With the advances in nanotechnology and nanosciences, a drastic change is observed in the field of material sciences. Being small in size and having a high surface area-to-volume ratio (SVR), nanoparticles have gained huge attention in the field of electronics, medicine, and environmental cleanup [1, 2]. Among all the nanoparticles, carbon-based nanoparticles like graphene and carbon nanotubes are most widely exploited for industrial applications. Currently, CNTs have overpowered all carbon and metallic-based nanoparticles due to their unique and remarkable properties like high mechanical

strength and lightweight [3]. Most of the synthesis techniques of CNTs are expensive due to the energy-intensive step. So, the scientific community is looking towards an alternate source of CNTs as a precursor material, for instance, coal fly ash (CFA), red mud, agricultural waste [4], plastic waste, and tires [5]. Most of these materials are waste of one industry and are easily available as a precursor material at a much more economical cost. So, the final product developed from such waste will also be cost-effective. The utilization of such waste-derived CNTs and carbon nanocomposites for environmental cleanup could prove to be much more economical.

Carbon nanotubes (CNTs) along with both single- and double-walled carbon nanotubes have left a notable impact. They have unique properties and were discovered in 1952 and 1976, respectively [6]. Since the discovery of CNTs in 1991 by the Japanese electron microscopist Sumino Iijima, a profound increase has been noted in the research and applications in this field [7]. CNTs are novel cylindrical hollow nanostructures that can be synthesized by both top-down and bottom-up approaches [8]. CNTs are made up of carbon atoms linked in a hexagonal shape, with each C-atom bonded to three other C-atoms by the covalent bond or a single sheet of pure graphite with a diameter of 0.7 to 50 nanometer (nm) [9]. The length of nanotubes may vary typically up to several microns [7]. With recent advancements in technology, the length of the nanotubes has been measured in centimeters also [10]. Research has been shifting towards the development of CNTs-based nanomaterials due to their advanced and unique chemical, electronic, mechanical, and structural features [11]. CNTs are built from graphene sheets having sp^2 carbon units, arranged in hexagonal networks [12]. CNTs are differing in length, thickness, structure, type of helicity, and number of layers [13]. CNTs show extraordinary properties with hardness almost equivalent to the diamond and thermal conductivity twice than that of pure diamond. According to their formation and types, nanotubes act either as metals or semiconductors [8]. According to their structure, CNTs are categorized as cylindrical shape and sometimes as pentagon structure with closed ends [5, 14], which are shown below in Table 1.

The authors have searched carbon nanotubes, carbon nanocomposites, and synthesis on science direct and found about more than 30000 articles, in the last five years, i.e., 2017-2022. There is continuous increase in the research on the CNTs which is evidenced by a huge number of articles in this field in recent years. In the year 2017, there were about 3283; in 2018, there were 3768; in 2019, there were 4453; in 2020, there were 5127; in 2021, there were 6546; and in year 2022 till August, there are about 6354 articles. CNTs has gained huge attention in the last few years. Out of all these 30000 articles in last five years, 16880 were alone research articles, followed by review articles which were 6431, 4256 as book chapters while rest were abstract, encyclopedia, and conferences. So, CNTs are one of the most widely focused material in the scientific community.

From the various articles, it has been found that due to high demand of CNTs and CNTs-based nanocomposites in the various fields like environmental cleanup, biomedicine, and electronics. The majority of synthesis are physical, like laser ablation, arc discharge method, and physical vapor deposition. Among chemical methods, chemical vapor deposition is most widely used. But most of these methods are expensive due to energy intensive process, i.e., reaction at high temperature. There are several reports where novel, innovative, ecofriendly, and economical approaches have been followed for the CNT synthesis. While among applications, it has been found that CNTs and their composites are widely used in the environmental cleanup like dye removal, heavy metal removal, antibiotic, and pesticide remediation from wastewater. Among medicines, it is widely used as a drug delivery agent for various anticancer drugs. After detailed investigation, all the applied techniques along with emerging ones are summarized over here.

The current review emphasizes on the current and emerging approaches for the synthesis of CNTs. Besides this, it also emphasizes on the potential of economical, biological, and industrial wastes as a source of raw material for the CNTs. The current and emerging applications of CNTs and nanocomposite are highlighted especially in the medicine, research, environmental clean-up, and electronics. The objective was to provide a summarized information about utilization of waste like agrowaste and industrial waste as an economical precursor source for the CNTs. Furthermore, utilization of waste for CNT synthesis will help in minimizing the solid wastes from the environment.

2. Recent Advances in the Synthesis Methods of CNTs

A number of physical, chemical, and electrochemical approaches have been used for nanotube synthesis [14]. Various types of precursors have been used for CNT development including acetylene, benzene, carbon monoxide, ethylene, and xylene [15]. CNTs have been synthesized by various physical and chemical methods for instance electrolysis, arc discharge, chemical vapor deposition (CVD) [15], sonochemical method, and laser ablation [16]. All these methods and their utilization for the synthesis of CNTs are given below in Figure 1.

2.1. Arc Discharge Method. Parkansky et al. synthesized MWCNT using single-pulse arc at room temperature. This method does not require any other kind of pretreatment. The sample is prepared using arc discharge between the target and counter electrode. Graphite plates, C-coated Cu grids, and Ni-coated glass slides are used in the reactor [17]. Wang et al. synthesized CNT using arc discharge in deionized water. A simple reactor is made using open vessel (1 l), graphite electrodes, and a DC power supply. Both anode and cathode are made of graphite and dipped in deionized water. After the arc discharge CNT is deposited on cathode. Black piece of CNT is collected for further examination. Within 60 seconds, the sample is prepared in the present study [18]. Wang et al. synthesized CNT using simple traditional direct current (DC) arc discharge reactor. Graphite tube, CuO powder, and graphite rod are used as consuming anode and cathode, respectively. Graphite tube is used as consuming anode and is filled with anthracite coal. The CuO-to-coal weight ratio is usually reported in the ration of 1 : 9. About 70 A and 20 V

Table 1: Categorization of CNTs and their size and synthesis method.

Carbon nanotubes	Size	Preparation method
Single-walled nanotubes (SWNTs)	0.4 to several nm in diameter	Laser ablation (LA), arc discharge (AD), chemical vapor deposition (CVD)
Double-walled nanotubes (DWNTs)	Interwall distance 0.33-0.42 nm	Arc discharge, peapod, and CVD
Multiwalled nanotubes (MWNTs)	Interwall distance approximate. 0.34 nm	Arc discharge, CVD, laser ablation, peapod method

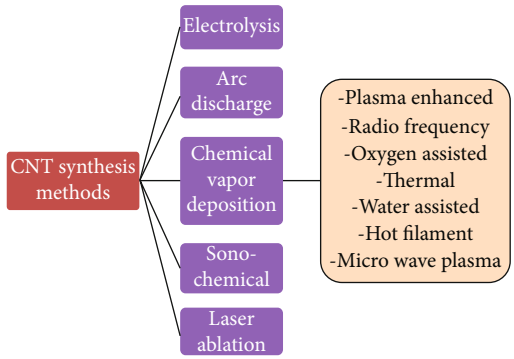

Figure 1: Methods for synthesis of CNTs and nanocomposite material.

DC voltage is applied as experimental conditions, respectively, in the current investigation. The AD is conducted for 15 minutes, and the final sample is collected from cathode [19]. Tsai et al. synthesized CNT using single-pulse discharge. The synthesis mechanism is based on microelectrodischarge method and is comprised of microelectrodischarge system. The applied voltage was 80 V, 2.0 A, and 2 μm, respectively. The electric current and discharging distance were also considered experimental conditions. Graphite electrode and substrate were used for microelectrodischarge system. A thin layer of Ni was used as a catalyst in the system. After single-pulse discharge, CNT was collected for further study. The experiment was carried out completely in an open atmosphere [20]. Zhao et al. synthesized CNT using alternate current (AC) arc discharge plasma. The experiment was carried out at normal atmospheric pressure. Experimental conditions were voltage and current at 380 V and 6 A–20 A, respectively. Tungsten electrode was used for the reactor preparation. Argon and benzene have been used as the plasma source and carbon source, respectively. Benzene was entered in the system using argon flow; simultaneously, argon and benzene were also introduced into the system. Finally, the arc discharge sample was collected on the internal wall of the reactor [21].

Su synthesized CNT using the one-pulse discharge method. The microelectrodischarge system was used for the synthesis in present investigation. The X–Y axis was used for position of discharging, and Z-axis was used to adjust the discharging distance. Peak currents (1.5, 2.0, and 2.5 A) and pulse durations (1200 and 1400 ms) were the experimental conditions used for the synthesis of CNT [22]. Maria and Mieno synthesized SWCNT using a low-frequency bipolar pulsed arc discharge method. They designed bipolar pulsed current circuit with constant current and constant pulse duration. Increased quantum efficiency was observed as compared to the unipolar pulsed arc discharge method. Two rectangular type C-Ni-Y electrodes were used in this study. He gas and 50 kPa pressure as experimental conditions were used for synthesis, and 0-5 Hz frequency was used for high quantum yield of synthesized material [23]. Berkmans et al. synthesized SWCNT using AD technique in open air. In the simple arc discharge setup, graphite was used as both the anode and cathode. A hole with measurement of Φ3 mm, and depth of 50 mm was made in the anode. This hole filled with 1 : 1 : 1 ratio of graphite, nickel, and yttria powders. Potential, direct current, power density, and current density were 36 V, 100 A, 3.8 kW/cm^2, and 105 A/cm^2 respective for experiment. After establishing, the arc discharge black fumes (CNT) was collected. The whole experiment was complete within 6 minute [24].

Arora and Sharma synthesized MWCNT from carbon black using AD technique. Two graphite electrodes were used for the construction of reactor. Anode having a hole and filled with carbon black was used. Graphite rod was used as cathode. After a 60-second arc discharge, the MWCNT was collected at the cathode [25]. Sun et al. synthesized CNT using AC arc and dielectric barrier discharge plasma. A simple AC arc plasma reactor with two sources were modified for the synthesis of CNTs. A mixture of propane and argon gas was injected into the preheated furnace. The furnace was made up of silicon nitride. In the simple procedure due to plasma generation, gaseous molecules were converted into positive and negative ions and neutral particles. During the synthesis, solid CNTs and gaseous byproducts were generated. CNT material was collected from the bottom of the container. Source can generate 20 kV and 20 to 40 kHz voltage and frequency range, respectively [26].

Riberio et al. reported the synthesis of CNTs by ADM, which was later on purified in order to remove the heavy metals, graphitized carbon, and amorphous carbon. Further analysis revealed that about 75% impurity was removed by adopting current techniques [27].

2.2. Laser Ablation (LA). Muñoz et al. worked on the role of gas and pressure on synthesis of single-walled carbon nanotubes. They used Ar, N, and He gases at 50-500 Torr pressure for conducting the experimental procedures. Continuous wave 10.6 μm CO_2–laser was applied for laser ablation. This laser was focused onto a graphite, Ni (4.2 at. %)/Y (1 at. %) composite target rod. The spot size and power density were measured to be 0.8 mm^2 and 0.8 mm^2, respectively [28].

Bolshakov et al. synthesized SWCNT using CW laser–powder method. A CW CO_2 laser (maximum output power of 2.1 kW, 2 aperture of 40 mm, and divergence of 4 mrad) was used for the ablation of graphite (carbon source). Laser focused on the mixture of graphite and metallic catalyst powders with the effect of argon and nitrogen gas. The gas sample was simultaneously collected from the lens using pure buffer [29]. Zhang et al. synthesized SWCNT using LA method at room temperature. Co/Ni (0.6/0.6 at %) as a catalyst and graphite powder were converted into plate target by heat treatment. Target was placed used 200-400 Torr pressure created by argon gas. Laser beam was focused on the target to obtain the CNT material [30].

Radhakrishnan et al. synthesized MWCNT using excimer laser ablation method. KrF laser (Lambda Physik 210 I, 248 nm, FWHM 25 ns, and laser intensity of 8×10^8 W/cm^2) has been used for synthesis, and 2 Torr gas pressure of oxygen and argon was controlled during preparation. The sample was collected at Si substrate [31]. Chrzanowskas et al. observed the effect of laser wavelength during the formation of CNTs by the LA method where laser-furnace reactor was used for synthesis with 6.6×10^4 Pa pressure under argon background was used in a quartz tube. Here, 1% graphite decorated with Ni and Co nanoparticles were placed in the quartz tube, and laser has been used for ablation. A quartz tube was placed in a preheated (1000°C) furnace. Double-pulse Nd:YAG Ekspla 303 D laser system was used for the irradiation purpose. This system generates two pulses with same wavelength. Effect of laser wavelength has been done using 355, 532, and 1064 nm wavelength [32]. Yuge et al. used CO_2 laser ablation method for synthesis of SWCNT at following operating conditions, i.e., 3.5 kW CO_2 laser was operated at 30×50 mm target rotating at 2 rpm for 30 sec. The sample was collected after some time. Boron- and nitrogen-doped SWCNTs were also prepared in this method. Gas pressure and flow rate have been controlled at 760 Torr and 10 l/min. The sample was prepared using argon and nitrogen atmosphere [33].

Alkallas et al. reported the synthesis of CNTs, decorated with NiO NPs by laser ablation technique. The synthesized materials were analyzed by the sophisticated instruments followed by its application for the remediation of methyl orange dye from wastewater. The developed nanocomposite have high adsorption capacity due to large surface area [34].

Mostafa et al. synthesized multiwalled CNTs decorated with Ag NPs by using laser ablation method in a liquid media. As per the investigators, the synthesis method was green as well as the one-pot method. The synthesized nanocomposite was used as a catalytic degradable agent for the nitrogen compounds and dyes. The synthesized NC has good catalytic activity and high distribution without utilizing any surfactant [3].

2.3. Chemical Vapor Deposition (CVD). Colomer et al. synthesized SWCNT using CCVD in a fixed-bed reactor. In this investigation MgO, methane, and mixture of methane/hydrogen were used as catalyst, carbon source, and carrier gas, respectively. After synthesis catalyst was removed using a concentration of hydrochloric acid and after purification, the sample was collected. The sample was prepared within 10 minutes using this method [35]. Scott et al. synthesized SWCNT using LA. In this method, graphite and cobalt/nickel system were used as the target and catalyst. Two Nd:YAG pulsed lasers were for ablation purpose operated at 532 nm and 1064 nm. The laser was operated on the target placed in the preheated furnace under argon environment created at 67 kPa [36]. Braidy et al. synthesized SWCNT using Nd:YAG laser vaporization method. In this method, three configurations of pulse at 532 nm, 1064 nm, and 532 nm with 1064 nm have been used for investigation. Target was prepared using graphite powder (2325 mesh), a C-cement, and Co–Ni powder catalyst (0.6% at.). The target was treated at 35 MPa and 800-1150°C in the presence of argon. The target mounted at quartz tube in preheated furnace was vaporized using pulse. After cooling, the sample was collected from the exit of the furnace [37].

Kokai et al. synthesized SWCNT using CO_2 laser vaporization. The target was prepared using graphite-Co/Ni (1.2 at. %). CO_2 laser beams (10.6 mm and 1 kW peak power) was used for the vaporization of the target material. The target was place in quartz glass situated at center of the preheated furnace. Simultaneously, argon gas was introduced in the furnace. After vaporization using CO_2 laser beam, the CNT was collected from the quartz glass plate [38]. Kokai et al. synthesized DWCNT using alumina-catalyzed CVD method. Methanol solution was used deposition of iron salt on an alumina support material. Flow of argon at 900°C temperature has initiated the process of CNT. After 10-minute, the sample was collected after cooling the reactor [38]. Qiu et al. synthesized SWCNT from coal gas using CVD. A horizontal quartz tube reactor was used for the synthesis. Two furnaces were also used in the system. In the first furnace, quartz boat having ferrocene catalyst was preheated (200°C) with coal gas. The second furnace was slowly heated and cooled after some time. After experiment, the black fiber-like materials deposited on quartz tube collected for further study [39]. Li et al. synthesized MWCNT using $MgMoO_4$-catalyzed CVD. Mg $(NO_3)_2 \cdot 6H_2O$ and $(NH4)6Mo_7O_{24} \cdot H_2O$ were used for the synthesis of $MgMoO_4$ catalyst. 1 g of $MgMoO_4$ catalyst was sprayed in a quartz boat put in a tube furnace at 1000°C. A mixture of methane/hydrogen gas was also used for synthesis [40]. Eftekhari et al. worked on the synthesis of MWCNT with cone-like heads using catalytic chemical vapor deposition (CCVD). Cobalt was used as the catalyst, and 1 : 1 ratio of barium chloride and calcium chloride was used as the catalyst support in the present investigation. Citric acid was also used as a foaming agent. All the chemicals were dissolved in water and dried at room temperature. The resultant product was a MWCNT with cone-like heads [41]. Terrado et al. synthesized MWCNT using thermal CVD. Quartz substrate was used to grow the CNT, and Co was used as a catalyst in the study. Different concentrations of cobalt nitrate in ethanol were sprayed on cleaned and sonicated quartz substrate under 1 bar pressure. At last, the sample was dried at room temperature. After that, the substrate was treated at 750–900°C in ambient condition and acetylene. Samples were collected after cooling the reactor [42]. Mckee et al. synthesized MWCNT using floating catalyst CVD method. Pyrolytic decomposition of a benzene-ferrocene has been responsible for the synthesis of CNT. In a

typical reactor, two furnace systems were used. The furnace was heated up to 750°C temperature. Argon and ferrocene–benzene was introduced into the preheated furnace. After some time, the CNT sample was collected on the substrate. Various operational parameters including catalyst concentration, growth time, and substrate type were also evaluated in the present investigation [43].

Shirazi et al. examined the role of various C-sources on the formation of MWCNT. The roles of cyclohexanol and xylene were evaluated on the synthesis method. Horizontal stainless-steel reactor was used in the study. About 1 : 20 molar ration of ferrocene and cyclohexanol or xylene was used as reagent. Evaporation of all the reagents has been done using oil bath [44]. Mubarak et al. synthesized CNTs using two-stage CVD by using ferrocene was used as the catalyst. Ceramic boat and two furnaces were used in the reactor where C_2H_2 was used as the carbon source. A catalyst was placed in a ceramic boat near the first furnace. The CNT was collected from the second furnace. A mixture of hydrogen/argon gas was also used in synthesis [45]. Hata et al. synthesized 99.98% pure SWCNT using water as the solvent. Ethylene and Ar or He with H_2 were also used in the synthesis. Fe nanoparticles and thin film were used as a catalyst on Si metal foil, quartz, and wafers in the present investigation. The synthesis method was completed in 10 min of reaction time [46].

2.4. Flame Method for the Synthesis of CNTs. Vander Wal and Ticich synthesized SWCNT and MWCNT using flame and furnace and performed a comparative study. In this study, Fe or Ni was used as the catalyst along with mixture of CO/H_2 and C_2H_2/H_2 with Fe to produce SWCNT and MWCNT. The CO/H_2 was used as a pyrolysis flame which was established after the addition of nanosized (catalyst) precursor particles as an aerosol. The aerosol was generated by drying a nebulized Fe or Fe colloid solution [47]. Yuan et al. synthesized MWCNT using ethylene flame. Stainless steel and cobalt–electrodeposited stainless-steel grid was used for synthesis. The stainless grid was heated with propane–air flame. Nitrogen was introduced to maintain the temperature of the system. The final product was obtained using nitrogen diluted–ethylene diffusion flame [48]. Yuan et al. synthesized MWCNT using methane flame. The stainless grid with Ni-Cr wire was used in this method. The final product was obtained using laminar co-flow methane-air diffusion flame [48]. Vander Wal et al. synthesized SWCNT using multistage flame configuration. The first-stage flame produces Fe catalyst, and CO, H_2, and He with air were used as a fuel-rich mixture in the first-stage flame. This fuel-rich mixture mixed with acetylene–air mixture comprised the second-stage flame. The Fe catalyst was used in the second-stage flame for the formation of SWCNT [49]. Saveliev et al. synthesized CNT using oxygen flame. 96%CH_4 with 4%C_2H_2, 50%O_2 with 50%N_2, and Ni-alloy (73%Ni+17%Cu+10%Fe) have been used as fuel, oxidizer, and catalyst. Fuel and oxidizer were mixed in the burner. Nitrogen gas was also introduced in the reactor during the burning process. After 10 minutes of reaction, CNT was collected [50]. Lee et al. synthesized MWCNT using an ethylene inverse diffusion flame. Air and C_2H_2 were utilized as an oxidizer and fuel, respectively. Pyrex glass chimney was used as the reactor. Stainless steel (304) plates and nickel nitrate were used as the target and catalyst. The substrate was kept near the flame, parallel to the flow [51].

Gore and Sane synthesized MWCNT using premixed flames. In this study, stainless steel (SS304) chimney was used for synthesis. Both the catalyst and target were made up of cobalt used. Both the catalyst and target were placed on molybdenum mesh holder at 1100°C temperature. Ethylene was used as a fuel [52]. Woo et al. synthesized CNT using double-faced wall stagnation flow burner. Mixture of ethylene (fuel), air, and nitrogen (diluent) gas were used for flame generation. Nickel-coated stainless steel target was used for synthesis. The target was heated for 3-10 minutes for CNT production [53].

Memon et al. synthesized MWCNT and SWCNT using counterflow diffusion flame (CDF) and multiple-inverse diffusion flames (m-IDFs). In the CDF method, $NiAl_2O_4$, $CoAl_2O_4$, and $ZnFe_2O_4$ spinels were used as the catalyst for synthesis. In this study, nitrogen-diluted methane was used as the fuel. Both nitrogen and methane are in 1 : 1 ratio. The copper substrate was inserted in to the system. After 10 minutes, CNT was collected. In m-IDF, same spinels were used as CDF. Methane or ethylene with hydrogen having 1 : 10 ratio was used as the fuel. The substrate temperature was maintained between 500 and 700°C [54].

2.5. Electrolysis Method for Synthesis of CNTs. Zhou et al. synthesized CNT using electrochemical deposition. The construction of the electrochemical reactor was done using an electrochemical cell with three chambers. For standard reference, they used calomel electrode and the anode and cathode were built using Fe/Ni alloy-coated nanoparticles. The electrode comprised of a mixture of 40 vol% methanol (CH_3OH) and 60 vol% benzyl alcohol ($C_6H_5CH_2OH$). About 1000 V potential difference has been maintained in the cathode and anode, and the CNT was obtained at cathode [55]. Johnson et al. synthesized CNT using from CO_2 by molten electrolysis. Molten lithium carbonate has been used for synthesis. Reaction was completed in pure alumina crucible. Different metals and nickel were used as the cathode and anode, respectively. During electrolysis, CNT and oxygen were formed on the cathode and anode, respectively. The synthesis procedure was completed in two steps—dissolution and electrolysis. In the dissolution process, lithium carbonate was synthesized. After this, lithium carbonate was converted in CNT [56]. Li et al. synthesized CNT using CO_2-based molten salt electrolysis. In this method, Li_2CO_3, $CaCO_3$, $SrCO_3$, and $BaCO_3$ were used for CNT preparation. Various combinations of these chemicals have been placed in a crucible and used for the synthesis. Galvanized iron wire and nickel wire were employed as the cathode and anode, respectively. Crucible was heated at 750°C temperature. Slowly, current density was increased from 6 mA/cm^2 to 200 mA/cm^2; as a result, CNT was deposited with increased current density [57].

2.6. Hydrothemal/Sonochemical Method for Synthesis of CNTs. Jeong et al. synthesize SWCNT using sonochemical method. Ferrocene (catalyst), p-xylene (carbon source),

and silica powder (nucleation site) were mixed together. After ultrasonication at ambient condition, CNT was collected [58]. Raja and Ryu synthesized CNT using sonochemical method. In a simple procedure, $ZnCl_2$ particles and dichlorobenzene were sonicated in ultrasonic water bath. 50 W/40 KHz is the maximum output of the system [59]. Wang et al. synthesized CNT using hydrothermal synthesis by utilizing precursor materials like ethyl alcohol, distilled water, sodium hydoxides (NaOH), and polyethylene glycol (PEG). These materials were mixed in a 250 ml flask. The reaction mixtures were continuously stirred for 30 minutes on a magnetic stirrer. After completion of 30 minutes, the precursor was transfected in a reactor for further treatment at 160°C for 20 h. After cooling, the sample was collected [60]. Razali et al. synthesized CNT using hydrothermal method. Ferrocene (2 g), sulfur (4 g), and NaOH solution (10 M) were used as carbon sources, catalyst, and solvent, respectively. The precursor was kept in Teflon stainless steel autoclave reactor at 200°C for 24 hours. After cooling, the sample was collected for further study [61].

2.7. Catalysis Method for Synthesis of CNTs. Kitiyanan et al. synthesized SWCNT using Co–Mo/SiO_2 catalyst. The investigators have used 1 : 2 molar ratio of Co–Mo. Cobalt nitrate and ammonium heptamolybdate used as a starting material in the present investigation. The starting material calcinated at 500°C placed in a horizontal quartz tubular reactor for further process. Precursor was then heated at 500°C and 700°C in H_2 and He atmospheres, respectively. After that, CO was introduced for the formation of the SWCNT material [62]. Liu et al. synthesized MWCNT using catalytic pyrolysis. In this method, polypropylene was converted into MWCNT which was accomplished in two steps. In the first step, catalytic pyrolysis and, second step, decomposition reaction have been carried out. HZSM-5 zeolite and nickel catalysts were used for synthesis. Screw kiln reactors were used for the first and second steps, respectively [63].

3. Agrowaste and Biochars as a Source of CNTs

Everyday, a huge number of agrowastes are generated around the whole globe, out of which some fractions are used as a fuel for burning, and some fractions are used as biomanures but major fractions are dumped into environment. Since these agrowastes small amount of water content which attracts the insects and microorganisms which causes pollution in the environment [64]. These agrowastes are rich in carbon which could act as an economical and ecofriendly material for the formation of CNTs by applying chemical, biological, and physical approaches. The utilization such agrowaste for this purpose will not only minimize the solid waste but also act an economical source of CNTs; hence, the final CNTs will be economical and ecofriendly [65]. There are several reports in the literature where agrowaste have been used for the generation of CNTs. Mugadza et al. synthesized CNTs from the sugarcane bagasse or cellulose in combination with ferrocene and ionic liquid. The diameter of CNTs 63 nm and 38 nm for sugarcane bagasse and cellulose, respectively, and used as a charged storage and numerous other applications [66]. The use of yeast fermented wheat flour for making CNT's was reported by Gao et al. [67]. He even used this to store energy. The CNTs produced using this method had a curved filamentous tabular structure with diameter between 100 and 200 nm. Another report suggested the use of agroindustrial waste such as wheat straw, hazelnut shell [68], coconut shell [69, 70], rapeseed cake, and oat hulls for synthesis of CNTs [71]. Here, the diameter of CNTs was inversely proportional to the energy band gap [72]. The following synthesis methods exhibit good potential for their applications in construction industries. Similarly, the use of poultry litter as raw material for synthesis of CNTs was studied by Haleem et al. [73]. The investigators reported the size of nanoparticles ranging between 26 and 200 nm in MWCNTs with well-aligned graphene walls. This method was further employed in the removal of chromium from wastewater during the tertiary treatment process [73].

Recently, Aboul-Enein et al. reported the synthesis of MW-CNTs from sugarcane bagasse. Here, the investigators used pyrolysis method for sugarcane bagasse (SCB), which was catalyzed by using zeolites. The investigators have used three different types of catalyst, namely, HZSM-5, HMOR, and HY. The temperature for pyrolysis was 450–700°C, while the SCB/ZSM-5 ratios were 3–12 [4].

3.1. Synthesis of CNTs from Biochar. Biochars are highly porous carbon-rich materials. They are obtained by the pyrolysis of substances of biological origin like coconut shell ash, corn cob, citrus peel waste, and rice husk ash [74]. Being rich in carbon, all these materials are the most suitable candidate for the synthesis of CNTs. Though there are several approaches for transformation of biological waste into biochars, the most preferred one is pyrolysis. Pyrolysis is considered advantageous over the biomass valorization processes. In this process, the waste can be handled in a much easier way and it also adds up to the sustainability of production processes.

There are numerous literatures which indicates the wider utility of these biochars especially in the soil. Since biochars are made up of organic carbon so even after burning, there is plenty of unburned carbon which could increase the organic carbon content in the soil. Moreover, due to highly porous nature, it could increase the water holding capacity of the soil, air aeration, and cation exchange capacity. It has also been found that these biochars could affect the soil pH based on their mineral content, i.e., could make the soil acidic or alkaline. Based on the mineral content, it could also affect the microbial community of the soil. Since biochars have various minerals which could act as a manure which could provide the nutrition to the soil for the growing plants, biochars has been used widely increase a sustainable alternative in the biomass valorization for value added product for instance adsorption or uptake of NH_4, NO_3^{2-}, Cd, phenols, production of Si compounds, and fulvic acids. Due to all these beneficial features, biochars has gained a huge response in the daily application in the field of agronomy and environmental purposes. Nowadays, it is widely used as a precursor material for the synthesis of CNTs by

microwave-assisted method, where it has numerous superiority due to low cost and ecofriendly nature. Such methods have numerous advantageous points as it minimizes the overall utilization of raw materials used for the CNT synthesis [72].

Recently, a novel technique for biochar-based CNTs with self-ignition solvent was designed. This solvent-based method gave high concentrations of CNTs when synthesized using horizontal furnace. It resulted in the release of high amount of energy from the autoignition solvent in the furnace. A higher degree of wall graphitization was also observed in the residual material. This method gave workable amount of lignocellulosic residual biomass and thus is a suitable applicator for agroindustries and construction industries. This new suggested technique for utilizing biochar as a source of black carbon for CNT production gives large quantities of purified CNTs [72].

Salama et al. synthesized environment friendly nanocompoosite fertilizer for common beans. The developed nanocomposite was based on CNTs which was developed from agricultural biochar [75].

4. Industrial Waste as a Source of CNTs

The conservationists all over the world are worried over the excessive accumulation of plastic waste in oceans, lakes, landfills, and rivers. The biggest concern relating to plastic waste is the lack of proper collection and recycling methods. This specific concern was acknowledged with novel approaches of utilizing CNTs in managing plastic waste.

Orbaek White et al. synthesized the CNTs from the chemical recycling of waste composite carbon source. The diameter of CNTs varied from 43 to 49.2 nm. The number of walls between 18 and 52 and diameter range between 18 and 45 nm. The synthesized CNTs used as a CNT cable for fuel savings because CNT cables are lightweight than the cable made from copper [76]. Li et al. synthesized CNTs from the polyethylene waste, and diameter and length was 20-30 nm and few tens of micrometers, respectively. Used as a field of composite materials were solar cells and optical devices [77]. Singh et al. synthesized CNTs from industrial waste, namely, fly ash, red mud, and rock sample, and used for the removal of methyl orange from aqueous medium. The diameter and length of CNTs was 20-30 nm and 683.8 nm, respectively [78]. Smagulova et al. synthesized CNTs from polymer waste and diameter range between 40 and 100 nm and used for obtaining various types of composite materials [79]. Yao et al. used the postconsumer waste plastics as a raw material for the production of CNTs and synthesized CNTs, mostly multiwalled and outer diameter from 12 to 25 nm. The synthesized CNTs have unique properties and number of applications in a wide variety of industries.

5. Synthesis of CNTs from Plastic Wastes

Plastic being nonbiodegradable is a major source of air, water, and soil pollution. It severely affects the natural environment. The use of plastic waste to synthesis CNTs using catalytic pyrolysis method is a novel as well as environment efficient method [80]. Here, the bimetallic Ni-Fe catalyst are used at a reaction temperature of 800°C to convert plastic waste into hydrogen and high-quality CNTs. A two-step method is used to fix the bed reactor where the plastic waste is first pyrolyzed and then is mixed along with various chemicals for further reactions. There are few factors that determines the quality of yield of CNTs from plastic waste like the development of reactor, quality of catalyst, and the conditions at which the operations are carried.

There are several examples in the literatures where plastic waste has been used for the synthesis of CNTs. Bazargan and McKay reported the synthesis of CNTS, single-walled, and multiwalled from various plastic wastes like polyethylene (HDPE or LDPE), polypropylene (PP), and polyethylene terephthalate (PET). They further said that such synthesis could be done in the autoclaves, furnaces reactors, and fluidized beds [81]. Zhuo reported the synthesis of CNTs from the waste polyethylene plastics. The yield of source of nanocarbon was up to 13.6%, and such approach will not only minimize the solid waste arising from the plastics but also provide an economical source of CNTs [82]. Wu et al. reported the synthesis of CNTs from the plastic waste by catalytic pyrolysis method by using NiMnAl catalysts. They observed that the higher the content of Mn in the NiMnAl catalyst, the more the yield of carbon (57.7 wt. %) from the plastic waste. Further, they prepared composite materials by adding 2% LPDE [82, 83].

The method followed most popularly after catalytic pyrolysis is microwave treatment for transforming the plastic waste into H and CNTs [84]. Recently, investigators from parts of the globe have developed catalytic method for converting plastic waste to better-quality fuel. Their methods comprise of pulverization of the plastic, where plastics were blended with tiny bits. This was followed by addition of ferrous oxides and aluminum oxide catalysts. Further, this mixture was a compedition to microwave treatment, where plastic catalysts were heated. This resulted in a catalyst which creates several hot spots in the plastic due to which almost 97% of the plastic's H, and high-quality CNTs was extracted. This novel process was reported superior over previously available techniques. These are less energy exhaustive, cheap, and single step process for fast production, i.e., within 30 to 90 seconds [85].

Smagulova et al. reported the synthesis of CNTs by CVD method where the polyethylene waste was thermally decomposed and were used were used as a carbon source. They observed the effect of decomposition temperature of polyethylene on the CNTs synthesis. Here, they impregnated the cenospheres with the aqueous solutions of nickel and cobalt nitrates. The latter was used as a catalyst for the synthesis of CNTs. They further concluded that for the synthesis of CNTs, optimum temperature for polyethylene decomposition was 450°C along with abovementioned catalytic conditions [84]. There are several reports where MWCNTs were also synthesized from the plastic waste which can eliminate or minimize the plastics from the environment. The plastic-based synthesized gelatin/MWCNT nanocomposite films was found water and oil resistant. Besides this, it also exhibited antimicrobial activity, due to

which it could be applied as a food packaging material. The coating of these nanocomposite materials with the garlic microparticles increases their antimicrobial activity. This resolves the toxicity-associated problem of MWCNTs during the process of migration. In the process of migration, an unintentional transfer of packaging material is carried on to the food. The use of garlic microparticles coated on the nanocomposite films helps in the avoidance of food interactions with the MWCNTs [85].

Pattanshetti et al. reported the synthesis of MWCNTs from waste plastic bottles by applying thermo-CVD method, and later on, the 30-45 nm diameter MWCNTs were analyzed by the X-ray diffraction (XRD), scanning electron microscopy (SEM), and electron diffraction X-ray (EDX) [86]. Further, a gelatin/MWCNT nanocomposite films was developed where garlic microparticles were synthesized by using the planetary ball milling method. Here, the percentage sof MWCNTs were varied from 1% to 3% to obtain different nanocomposites [86]. In a study, Tripathi et al. synthesized MWCNTs in the laboratory using used polypropylene centrifuge tubes [87]. The process of synthesis involved the use of double-layered stainless steel 316 (SS 316) metal tube. This dual layer acts both as the vessel for the reactor and as catalyst. The steal reactor is mixed up with Fe and sometimes Ni. This helps in the conversion of carbon that will be used for analysis by spectroscopic, microscopic, and thermogravimetric method. With the following experimentation, the optimum condition for reaction was concluded at 900°C under normal reaction conditions [87].

Most recently, Ramzan et al. synthesized CNTs in single step by using plastic waste as a precursor. The method adopted by investigators was microwave assisted by using various catalyst like $NiFe_2O_4$, Al_2O_3, and Fe_2O_3 which was synthesized by sol-gel technique. The investigation focused on the valorization of plastic and its transformation into CNTs [88].

6. Current and Emerging Applications of CNTs

Due to the light weight, high mechanical strength, unique electronic, and thermal features, CNTs have gained attention in the field of electronics, sensors, defense, biomedical, drug delivery, and environmental cleanup [89, 90]. Among electronics, it is widely used in batteries for efficient energy storage applications [91].

6.1. CNT for Energy Storage Applications. Whereas the durability and specific energy distribution of double-layered capacitive substances such as CNTs have been established and appreciated, the power output constraint has drawn a lot of interest. When superior electron capacitive components like graphene, activated carbon, metal oxide, transition sulfide, or conducting polymers are combined with carbon nanotube-oriented fibers, the conductivity of the native fibers can be greatly increased by maintaining the periodic features [92]. In this context, Peng et al. constructed a CNT/graphene composite fiber by covering the as-prepared MWNT assemblies with GO colloidal and spinning them into fibers. The transfer tendency of electrons in the composite fiber is noticeably enhanced because of contact of the pi-pi bond between the graphene oxide sheet and the carbon nanotube, and the graphene oxide layer can reduce carbon nanotube packing and enhance ion pathways. In comparison to naked CNT fiber (630 MPa), the chemical-reduced blended fiber seems to have a mechanical property of 500 MPa, whereas the conductance of the fiber reinforcement can be as strong as 450 20 S/cm. In comparison to the 5.83 F/g of the pure CNT fiber, the mixed fiber's computed specific capacity was 31.5 F/g, while Foroughi et al. investigated a unique type of inductive carbon nanotube-graphene hybrid fiber under electrospinning chemical-reduced graphene within and covering the face of MWNT fiber during the drawing phase, based on a similar principle. The functionalized fiber had electrical properties of 900 50 S/cm, whereas its impact resistance, stiffness, and modulus of rupture were all about 140 MPa, 2.58 GPa, and 6%, correspondingly. At a scanning speed of 2 mV/s, the specific capacity was considerably enhanced to 111 F/g. The cospun CNT-based fiber could also improve the fundamental electrocatalytic activity as a comparison to the naked CNT fiber with the use of nanocrystals or nanoflakes [93]. Di et al. used a spinnable CNT array to paint a suspension of ordered microporous carbon (OMG) over 10 sheets of ordered CNT layers, which were then wrapped together into fiber concrete as one electrode [94]. Even at a scanning speed of 200 mV/s, the electrochemical behavior of the OMC/CNT hybrid fiber was tested in a three-electrode system, which revealed a rectangular-shaped CV curve. The particular volumetric capacitance of the produced negative electrode was up to 121.4 F/cm^3 (or 116.3 F/g) at 0.43 A/cm^3, which was regulated mostly by the amount of OMC particles in the hybrid fiber composite (76 wt%). Apart from conducting polyaniline, polypyrrole (PPy) was been found to have higher superior catalytic properties. Using two or more pieces of stainless-steel mesh as the working electrode, Di et al. successfully deposited a light coating of PPy on an aligned CNT sheet [94]. Two motors with direction opposite coiled the layered coatings into fibers in a wet condition. The as-prepared fiber electrode then demonstrated high capacitance (350 F/g) and remarkable durability in cyclic measurement, even when bent and twisted.

6.2. CNTs for Environmental Applications. Active atomic surfaces of polymeric structure CNTs have been already emerged to improve the adsorption and catalytic performance with respect to eliminate heavy ions and heterocyclic complexes. However, the hybrid structural characteristics of the CNTs materials were found more efficient towards environmental issues like dye degradation, metal adsorption, and water purifications from the wastewater contaminants [95]. In this regard, Adam et al. prepared novel metal–carbon-based catalysts for the adsorption of (Hg(II), Pb(II), Cd(II), and Sn(II) ions) heavy ions from an aqueous media. Here, the interfacial bond structures between the heavy metals and the $ZnFe_2O_4$ combination boost the adsorption ability of free fullerene CNT towards the examined toxic metal ions by 25% when homogenized with the $ZnFe_2O_4$ composition. The removal efficiency of various heavy metals is shown below in Figure 2. It is noted that the fullerenes are effective substances for the recovery of pollution from wastewater

because of their flaws, reduced agglomeration propensity, and extensive surface sites [96].

ZnO/NiO supported MWCNTs were magnificently made up by coprecipitation technique by Khan et al. [97], and the degradation of methyl orange (azo dye) was examined under UV and visible illumination to estimate the photocatalytic performance of the photocatalyst as produced. Once NiO was deposited on the MWCNTs with a ZnO-coated layer, the reactivity increased even further, peaking at 3% NiO concentration. The decay behavior of ZnO-encased MWNTs and ZnO/NiO-covered MWCNTs differed, implying that comprehensive degradation of organic azo dyes can be obtained under rapid catalyzed decomposition processes when ZnO/NiO-treated MWCNTs are used. By hydrolyzing titanium isopropoxide in saturated alcohol, Jiang and Gao [98] had shaped TiO_2- (anatase-) loaded MWCNT nanocatalysts. On visible spectrum, phenol was decomposed, and the composites had greater potency (92.4 percent in 8 hours) than undoped TiO_2 and a mixed combination of MWCNTs and TiO_2, which is shown in Figure 3.

6.3. Applications of CNTs in Biomedical. It is generally understood that the CNTs have a fundamental atomic chemistry and phase purity influence interface attributes including polarity, wettability or high porosity, dispersion, and catalytic activities. This will influence the contacts itself with surroundings, particularly biomolecule adhesion. In the imaging subject area, there are a variety of CNT-based approaches. Photoluminescent imaging, for example, uses the fluorescence of activated SWCNT on near infrared-I and NIR-II spectrum, which are practically opaque to biomolecules and fluids, allowing for depth penetration properties [70, 99]. Conductive detectors, and more specifically differential resistive pulse devices constructed on MWCNT, have successfully demonstrated their usefulness in achieving single molecule information [100]. These refer to possible medical impacts wherein CNTs are used to optimize the functionality of established hospital devices rather than to generate new nano-based technologies.

7. Nanocomposite Material and Their Applications

Nanocomposite is a medium where the nanoparticles adhere to and improve the property of material [101]. The solid multiphase material has three dimensions with an average size lesser than 100 nm. Nanocomposite has become the backbone of all the scientific industries due to their advanced mechanical, electrical, thermal, optical, catalytic, and electrochemical properties, which make them remarkably differ from that of component materials [102]. Because of these properties, CNT metal matrix composites are growing as new materials and are also applied to solve environmental problems. Nowadays, nanocomposites are widely used in environmental cleanup, biomedicine, ceramics, defense, and aerospace [103].

7.1. Energy Storage and Electrical Conductivity. Energy storage nanocomposite has been produced by Chanchal et al. using Mn_3O_4 nanoparticles having the size of about 60 nm

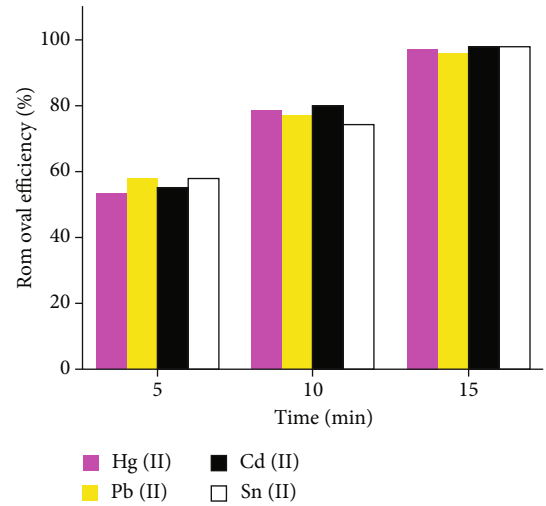

Figure 2: Heavy metal removal profile from aqueous solution (percentage) utilizing 50 mg of produced $ZnFe_2O_4$-CNT adsorbent material at various contact durations [96].

diameter and conductive MWCNTs. Thus, developed nanocomposite material shows the high value of specific capacitance, power density, and energy density. MWCNT/Mn_3O_4 nanocomposite was synthesized using modified hydrothermal (MHT) route. MWCNTs has increased conductivity and reduction in the charge transfer process because of its natural porous and conductive nature. According to GCD test, researchers had concluded that 8.5 wt% MWCNT/Mn_3O_4 nanocomposite represents the highest capacitance of 396 F g^{-1} at 1 A g^{-1} current density. This is 1.4 times higher than bare Mn_3O_4 with specific capacitor of 264 F g^{-1}. Researchers had also stated that nanocomposite shows enhanced cyclic stability, which makes a resourceful supercapacitor electrode material [104]. Another study based on electrical conductivity was carried out by Patole and Lubineau [105]. In their, they have used silver nanoparticles decorated ethylenediamine (EDA) functionalized MWCNT-EDA. The conductive layer of ethylene glycol treated poly(3, 4-ethelenedioxythiophene): poly(styrenesulfonate) (PEDOT: PSS) was used for Ag/MWCNT-EDA coating [105]. Researchers found that EP coating enhances the electrical conductivity of developed a nanocomposite material in two ways. The EP coating acts as an effectual scattering agent that enhances the equal dispersion of the Ag/MWCNT-EDA. The use of EP coating is also seen as a mutual bridge among Ag and MWCNT-EDA.

Kiani et al. have developed and characterized polythiophene/SWCNTs nanocomposite which shows advanced improved electrical conductivity and thermal stability. They have taken thiophene (Th) and 2-(2-thienyl) pyrrole (TP) as an interfacial modifier for the development of SWNT-poly (Th-TP) nanocomposite [106]. The characterization of nanocomposite materials was carried with sophisticated instruments such as UV-visible spectroscopy, Fourier transform infrared spectroscopy (FTIR), Raman spectroscopy, field emission scanning electron microscopy (FE-SEM), thermogravimetric analysis (TGA), XRD, transmission

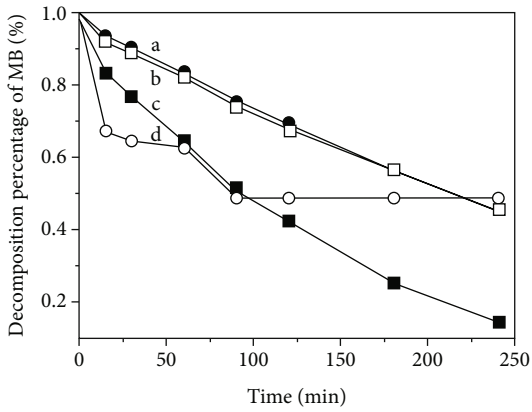

FIGURE 3: Destruction of MB by (a) ZnO nanostructures, (b) MWNTs and ZnO combinations, (c) ZnO-based MWNTs composites, and (d) MWNTs.

electron microscopy (TEM), and scanning tunneling microscopy (STM). According to characterization date, thiophene and TP molecules are adsorbed onto the surface of hybrid SWNTs where SWNT constitutes the core and poly (Th-TP) acts as the shell. The developed nanocomposite material shows improved thermogravimetric stability along with electrical conductivity as large as 28 Scm^{-1} which is much larger than the usual value of bulk poly (Th-TP).

Another work on enhanced electrical conductivity is based on nanocomposite developed using few-walled carbon nanotubes (FW-CNTs) decorated with palladium nanoparticles as fillers. During the nanocomposite synthesis, the FW-CNTs were initially adhered by the Pd and $PdCl_2$ particles, after the reduction process in dihydrogen, all the decorated particles on the surface of FW-CNTs were transferred to spherical Pd nanoparticles with average diameter of 5 nm. Thus, the developed nanocomposite material provide additional channels for electron transfer and also decrease the contact resistance due to p-type doping effect and the decrease in the SBH, which subsequently increase the electrical conductivity of nanocomposite material [107].

In recent times, electronic devices such as communication devices, touch screens, surgical, nd diagnostic implements are used widely. Designing a more flexible electrochemical energy storage is tremendously important for the growing demand of flexible devices. These days' lithium-ion batteries (LiBs) and supercapacitors (SCs) are growing as typical energy devices. Incorporation of nanomaterials in such devices enhances their capacity and efficiency, due to advanced properties of nanomaterials. Yin et al. have used nano-based approach to assembling hybrid energy storage devices. In their study, the flexible, ultrathin, and low weight carbon nanotubes-polyaniline (CNT/PANI) composite films were developed and used as supercapacitor electrodes. Developed nanocomposite materials were directly introduced into a lead acid battery in series or parallel. The hybrid devices on the other hand showed better properties. There was an increase in 19% specific capacity and 21% in specific energy [108]. The wearable electronic gadgets are in high demand these days and to fulfil the demand. Wang et al. have designed fiber-shaped energy storage device. These devices can be woven into electronic textiles. The study showed that a coaxial fiber lithium-ion battery can be done by adding aligned carbon nanotube composite yarn. Designed novel nano-based material show good results with a linear energy density of 0.75 $mWh\,cm^{-1}$. A wearable energy storage textile has been produced by researchers with an aerial energy density of 4.5 0.75 $mWh\,cm^{-2}$ [109].

7.2. Thermal Conductivity. Carbon nanotubes incorporated with polyester/vinyl ester resins and infusion with glass fiber lead to the development of carbon nanotubes/glass fiber/polymer multiscale composite using ultrasonic process and shearing. In this study, the addition of just 3% of carbon nanotubes has resulted in 1.5-fold enhancement of thermal conductivity [110]. Researched had stated that the ultralow thermal conductivity of bulk polymer such as polythene can be enhanced by combining them with nanomaterials which are having high thermal conductivity. They have developed aligned carbon nanotube polythene composites (ACPCs). The most interesting and significant finding is that developed ACPCs nanocomposite material twice thermal conductivity as large as a suspended PE chain which is well known by its high K. As compared to reported CNT-polymer composites, the K ACPC is also at least 30 times higher, and due to these advanced properties, Liao et al. has predicted that aligned polymer-based composites may be used for wide variety of applications [111]. Another research study on carbon nanotube copper (CNT/Cu) has been carried by Chu et al. They have synthesized CNT/Cu nanocomposite using a novel particles-compositing process followed by spark plasma sintering (SPS) technique. They reported that sintering condition affects the thermal conductivity, i.e., the composite material sintered at 600°C for 5 min under 50 MPa pressure showed maximum thermal conductivity, while sintering at below 600°C and below 50 MPa pressure, thermal conductivity decreases. According to experimental data, they have concluded that the increases in both temperature and pressure enhanced the thermal conductivity of CNT/Cu composite [112]. To characterize the thermal conductivity, Kong et al. had incorporated CNTs into the Cu-Cr matrix and fabricated CNT/Cu-Cr composite. They had used powder metallurgy method which consists of ball milling of CNTs with matrix powder followed by hot processing during their study. High-resolution transmission electron microscopy was used to detect Cr_3C_2 carbide layer. The carbide layer increases the interfacial bonding because of its strong chemical bond. The heat transfer between the CNT and the Cu-Cr matrix is also improved. A significant increase of nearly 12-17% in thermal conductivity was reported in the study when compared to the Cu-Cr matrix with the CNT loading of 5 vol. % and 10 vol. %, respectively [113].

7.3. CNTs as Sensor. CNTs incorporated with different materials such as polymers, nanoparticles, and the bulk material shows advanced sensing properties. Indium oxide was grown on the surface of oxidized SWCNT to develop nanocomposite material using sol-gel synthesis method. Synthesized hybrid nanocomposite reveals high conductivity and sensitivity toward certain organic vapors at room temperature. To check

the sensing properties of indium oxide/SWCNT hybrid nanomaterials, an electrical conductance experiment was carried out for dilute ethanol and acetone vapors. They have also observed that as the degree of annealing greatly affects the material's response to acetone and ethanol, the intermediate calcinations condition yields the best sensitivity [114]. Qualitative and quantitative monitoring of harmful and hazardous gasses such as carbon monoxide (CO), nitrous oxide (NO), and nitrogen dioxide (NO_2) is of great importance in several application areas such as environmental pollution [114]. To overcome this problem, Sekhaneh and Dahmani have synthesized SWCNTs/ZNO nanocomposite for nitrogen dioxide (NO_2) detection at room temperature. As compared to SWCNT sensor, SWCNTs/ZNO nanocomposite sensor shows much interesting and impressive response at the temperature higher than 100°C and they are also having high sensitivity to NO_2 concentration as low as 1 ppm. In another study, Mendoza et al. have developed tin oxide carbon nanotubes (SnO_2-CNTs) composite by chemical vapor deposition method (CVD), which shows sensitivity against methanol, ethanol, and hydrogen sulfide (H_2S). As compared to SnO_2 and CNTs separately, SnO_2-CNTs composite shows advanced and efficient performance to ppm level of gas. Researched have stated that the developed nanocomposite material may be used as road alcoholmeters and industrial safety [115].

7.4. CNTs as Catalyst. The science of catalysis and their technology is very significant to a national economy. Today, about 90% of all the technical chemicals are manufactured by the use of catalysts. Due to a higher surface area-to-volume ratio, metal nanoparticles are highly important material as catalysts [116]. Nanosized titanium dioxide has gained considerable attention due to its novel properties, which include chemical stability, nontoxicity, large specific surface area, and high photocatalytic activity. Due to its exceptional properties, they show a broad range of applications, such as dye-synthesized solar cells, water splitting, and environmental applications. Researchers have reported that incorporation of CNTs with titanium dioxide enhanced its photocatalytic activity [117]. During their work, titania nanotubes (TNTs) were prepared by electrochemical anodization technique. CNTs were synthesized inside the titania nanotubes (TNTs) templates by a catalyst-free chemical vapor deposition (CVD) method. The synthesized CNT-TNT nanocomposite was characterized using Raman spectroscopy, SEM, transmission electron microscope (TEM), XRD, and X-ray positron spectroscopy (XPS). Characterization data reveals that the size of TNTs was found ~100 nm pore diameter and the thickness of CNTs were 4 ± 2 nm. Developed nanocomposite was used to remediate Rhodamine B dye. Researchers concluded that CNTs induce synergetic effects on the photocatalytic activity of TNTs, which enhanced Rhodamine B degradation [118]. In another study, researchers have developed nitrogen-doped carbon nanotube/nanoparticle (N-Fe-CNT/CNP) nanocomposite which possesses electrocatalytic activity for oxygen reduction reaction (ORR) in alkaline medium. The developed nanocomposite shows higher efficiency than platinum- (Pt-) based catalyst [119].

7.5. CNTs as Heavy Metal Adsorbent. Heavy metals are widely used in industrial purpose which includes painting and battery manufacturing [120]. Industrial processing results in the generation of large quantities of waste effluent that contains exceed the level of heavy metals [121]. Most of the heavy metals are very toxic which cause cancer. They are also nonbiodegradable and persist in the aquatic ecosystem and environment which affect living beings. To solve such problems, Sankararamakrishan et al. have carried out to study the adsorption properties of carbon nanotubes and activated alumina nanocomposite. Chemical vapor deposition technique was used to grow carbon nanotubes over Fe- and Ni-doped activated alumina. The next step involved washing of nanofloral clusters with acid. This nanoparticles can be used for absorption of Cr(VI) and Cd(II) in the pH of 2 and 9, respectively. The adsorption equilibrium data were best fitted by the Langmuir model. According to Van't Hoff equation, the adsorption process is irreversible, stable, and feasible. As the developed NCs shows respective properties, researchers have concluded it as the unique adsorbent for cleaning up the environment. Generally, alginate and carbon nanotubes both are used as an adsorbent material [122]. Jeon et al. have taken this advantage and prepared a nanocomposite material using alginate, carbon nanotubes, and iron (III) oxide for the removal Cu(II) [123]. Iron oxide shows the respectable property for recovery after the removal of heavy metal to eliminate the secondary pollution. SEM and TEM data reveals that addition of CNTs enhanced the surface area for heavy metal adsorption. Developed nanocomposite showed about 60% enhanced recovery of Cu(II) which shows very impressive properties of the nanocomposite material [123]. In another study, iron oxide magnetic nanoparticles were incorporated along with multiwalled carbon nanotubes to prepare multiwalled carbon nanotube/iron oxide magnetic (MWCNTs/Fe_2O_3) nanocomposite for the removal of Ni(II) and Sr(II) contamination. Formation of the nanocomposite was confirmed by SEM analysis. Researchers had also concluded that pH and ionic strength affect the activity of nanocomposite for heavy metal adsorption [124].

8. Conclusion

Agrowastes could act as a potential candidate for the synthesis of economical and ecofriendly CNTs and nanocomposites. The utilization of agrowastes has resulted in the minimization of the solid waste and diseases arising from the disposal of wet agrowastes. Till yet, all the three approaches, i.e., biological, chemical, and physical, have been successfully applied for the synthesis of CNTs and nanocomposites. Since the CNTs are developed from agrowastes, these were biocompatible. Applications of CNTs have gained importance in the field of sensors, adsorbent, defense, and aerospace engineering. It has also gained wider applications in the biomedical field mainly prosthetics and stents which are very light and high durability. The utilization of agrowaste and development of CNTS will help in minimization of waste generated from agricultural activities around the globe every year.

Data Availability

The data sets used and analyzed during the current study are available within the article only.

Conflicts of Interest

All authors declare that there is no conflict of interest associated with this research work either in terms of financial or employment.

Authors' Contributions

Amel Gacem, Shreya Modi, and Virendra Kumar Yadav contributed equally to this work and are considered co-first author.

References

[1] V. K. Yadav, N. Choudhary, S. H. Khan et al., "Synthesis and characterisation of nano-biosorbents and their applications for waste water treatment," in *Handbook of Research on Emerging Developments and Environmental Impacts of Ecological Chemistry*, G. Duca and A. Vaseashta, Eds., pp. 252–290, IGI Global, Hershey, PA, USA, 2020.

[2] N. Choudhary, V. K. Yadav, P. Malik et al., "Recovery of natural nanostructured minerals: ferrospheres, plerospheres, cenospheres, and carbonaceous particles from fly ash," in *Handbook of Research on Emerging Developments and Environmental Impacts of Ecological Chemistry*, G. Duca and A. Vaseashta, Eds., pp. 450–470, IGI Global, Hershey, PA, USA, 2020.

[3] A. M. Mostafa, E. A. Mwafy, N. S. Awwad, and H. A. Ibrahium, "Synthesis of multi-walled carbon nanotubes decorated with silver metallic nanoparticles as a catalytic degradable material via pulsed laser ablation in liquid media," *Colloids and Surfaces A: Physicochemical and Engineering Aspects*, vol. 626, p. 126992, 2021.

[4] A. A. Aboul-Enein, A. E. Awadallah, D. S. El-Desouki, and N. A. K. Aboul-Gheit, "Catalytic pyrolysis of sugarcane bagasse by zeolite catalyst for the production of multi-walled carbon nanotubes," *Journal of Fuel Chemistry and Technology*, vol. 49, no. 10, pp. 1421–1434, 2021.

[5] J. Alam, V. K. Yadav, K. K. Yadav et al., "Recent advances in methods for the recovery of carbon nanominerals and polyaromatic hydrocarbons from coal fly ash and their emerging applications," *Crystals*, vol. 11, no. 2, p. 88, 2021.

[6] L. S. Salah, N. Ouslimani, D. Bousba, I. Huynen, Y. Danlée, and H. Aksas, "Carbon nanotubes (CNTs) from synthesis to functionalized (CNTs) using conventional and new chemical approaches," *Journal of Nanomaterials*, vol. 2021, Article ID 4972770, 31 pages, 2021.

[7] M. Thiruvengadam, G. Rajakumar, V. Swetha et al., "Recent insights and multifactorial applications of carbon nanotubes," *Micromachines*, vol. 12, no. 12, p. 1502, 2021.

[8] N. Baig, I. Kammakakam, and W. Falath, "Nanomaterials: a review of synthesis methods, properties, recent progress, and challenges," *Materials Advances*, vol. 2, no. 6, pp. 1821–1871, 2021.

[9] N. Saifuddin, A. Z. Raziah, and A. R. Junizah, "Carbon nanotubes: a review on structure and their interaction with proteins," *Journal of Chemistry*, vol. 2013, Article ID 676815, 18 pages, 2013.

[10] T. Zhou, Y. Niu, Z. Li et al., "The synergetic relationship between the length and orientation of carbon nanotubes in direct spinning of high-strength carbon nanotube fibers," *Materials & Design*, vol. 203, p. 109557, 2021.

[11] M. Rahamathulla, R. R. Bhosale, R. A. M. Osmani et al., "Carbon nanotubes: current perspectives on diverse applications in targeted drug delivery and therapies," *Materials (Basel)*, vol. 14, no. 21, p. 6707, 2021.

[12] A. Armano and S. Agnello, "Two-dimensional carbon: a review of synthesis methods, and electronic, optical, and vibrational properties of single-layer graphene," *Journal of Carbon Research*, vol. 5, no. 4, p. 67, 2019.

[13] A. Garg, H. D. Chalak, M. O. Belarbi, A. M. Zenkour, and R. Sahoo, "Estimation of carbon nanotubes and their applications as reinforcing composite materials-an engineering review," *Composite Structures*, vol. 272, p. 114234, 2021.

[14] S. Modi, R. Prajapati, G. K. Inwati et al., "Recent trends in fascinating applications of nanotechnology in allied health sciences," *Crystals*, vol. 12, no. 1, p. 39, 2022.

[15] B. Yang, L. Gao, M. Xue et al., "Experimental and simulation research on the preparation of carbon nano-materials by chemical vapor deposition," *Materials (Basel)*, vol. 14, no. 23, p. 7356, 2021.

[16] A. Szabó, C. Perri, A. Csató, G. Giordano, D. Vuono, and J. B. Nagy, "Synthesis methods of carbon nanotubes and related materials," *Materials*, vol. 3, pp. 3092–3140, 2010.

[17] N. Parkansky, R. L. Boxman, B. Alterkop, I. Zontag, Y. Lereah, and Z. Barkay, "Single-pulse arc production of carbon nanotubes in ambient air," *Journal of Physics D: Applied Physics*, vol. 37, no. 19, pp. 2715–2719, 2004.

[18] S.-D. Wang, M.-H. Chang, J.-J. Cheng, H.-K. Chang, and K. M.-D. Lan, "Unusual morphologies of carbon nanoparticles obtained by arc discharge in deionized water," *Carbon*, vol. 43, no. 6, pp. 1322–1325, 2005.

[19] Z. Wang, Z. Zhao, and J. Qiu, "Synthesis of branched carbon nanotubes from coal," *Carbon*, vol. 44, no. 7, pp. 1321–1324, 2006.

[20] Y. Y. Tsai, J. S. Su, C. Y. Su, and W. H. He, "Production of carbon nanotubes by single-pulse discharge in air," *Journal of Materials Processing Technology*, vol. 209, no. 9, pp. 4413–4416, 2009.

[21] S. Zhao, R. Hong, Z. Luo, H. Lu, and B. Yan, "Carbon nanostructures production by AC arc discharge plasma process at atmospheric pressure," *Journal of Nanomaterials*, vol. 2011, Article ID 346206, 6 pages, 2011.

[22] J.-S. Su, "Direct route to grow CNTs by micro-electrodischarge machining without catalyst in open air," *Materials and Manufacturing Processes*, vol. 25, no. 12, pp. 1432–1436, 2010.

[23] K. H. Maria and T. Mieno, "Synthesis of single-walled carbon nanotubes by low-frequency bipolar pulsed arc discharge method," *Vacuum*, vol. 113, pp. 11–18, 2015.

[24] J. Berkmans, M. Jagannatham, R. Reddy, and P. Haridoss, "Synthesis of thin bundled single walled carbon nanotubes and nanohorn hybrids by arc discharge technique in open air atmosphere," *Diamond and Related Materials*, vol. 55, pp. 12–15, 2015.

[25] N. Arora and N. N. Sharma, "Effect of current variation on carbon black to synthesize MWCNTs using pulsed arc

discharge method," *Materials Today: Proceedings*, vol. 4, no. 9, pp. 9394–9398, 2017.

[26] D. L. Sun, R. Y. Hong, F. Wang, J. Y. Liu, and M. Rajesh Kumar, "Synthesis and modification of carbon nanomaterials via AC arc and dielectric barrier discharge plasma," *Chemical Engineering Journal*, vol. 283, pp. 9–20, 2016.

[27] H. Ribeiro, M. C. Schnitzler, W. M. da Silva, and A. P. Santos, "Purification of carbon nanotubes produced by the electric arc-discharge method," *Surfaces and Interfaces*, vol. 26, p. 101389, 2021.

[28] E. Muñoz, W. K. Maser, A. M. Benito et al., "Gas and pressure effects on the production of single-walled carbon nanotubes by laser ablation," *Carbon*, vol. 38, no. 10, pp. 1445–1451, 2000.

[29] A. P. Bolshakov, S. A. Uglov, A. V. Saveliev et al., "A novel CW laser-powder method of carbon single-wall nanotubes production," *Diamond & Related Materials*, vol. 11, no. 3-6, pp. 927–930, 2002.

[30] H. Zhang, Y. Ding, C. Wu et al., "The effect of laser power on the formation of carbon nanotubes prepared in CO_2 continuous wave laser ablation at room temperature," *Physica B: Condensed Matter*, vol. 325, pp. 224–229, 2003.

[31] G. Radhakrishnan, P. M. Adams, and L. S. Bernstein, "Room-temperature deposition of carbon nanomaterials by excimer laser ablation," *Thin Solid Films*, vol. 515, no. 3, pp. 1142–1146, 2006.

[32] J. Chrzanowska, J. Hoffman, A. Małolepszy et al., "Synthesis of carbon nanotubes by the laser ablation method: effect of laser wavelength," *Physica Status Solidi (b)*, vol. 252, no. 8, pp. 1860–1867, 2015.

[33] R. Yuge, F. Nihey, K. Toyama, and M. Yudasaka, "Preparation and characterization of newly discovered fibrous aggregates of single-walled carbon nanohorns," *Advanced Materials*, vol. 28, no. 33, pp. 7174–7177, 2016.

[34] F. H. Alkallas, A. Toghan, H. A. Ahmed et al., "Catalytic performance of NiO nanoparticles decorated carbon nanotubes via one- pot laser ablation method against methyl orange dye," *Journal of Materials Research and Technology*, vol. 18, pp. 3336–3346, 2022.

[35] J. F. Colomer, C. Stephan, S. Lefrant et al., "Large-scale synthesis of single-wall carbon nanotubes by catalytic chemical vapor deposition (CCVD) method," *Chemical Physics Letters*, vol. 317, no. 1-2, pp. 83–89, 2000.

[36] C. D. Scott, S. Arepalli, P. Nikolaev, and R. E. Smalley, "Growth mechanisms for single-wall carbon nanotubes in a laser-ablation process," *Applied Physics A*, vol. 72, no. 5, pp. 573–580, 2001.

[37] N. Braidy, M. A. El Khakani, and G. A. Botton, "Single-wall carbon nanotubes synthesis by means of UV laser vaporization," *Chemical Physics Letters*, vol. 354, no. 1-2, pp. 88–92, 2002.

[38] F. Kokai, K. Takahashi, M. Yudasaka, R. Yamada, T. Ichihashi, and S. Iijima, "Growth dynamics of single-wall carbon nanotubes synthesized by CO_2 laser vaporization," *The Journal of Physical Chemistry B*, vol. 103, no. 21, pp. 4346–4351, 1999.

[39] J. Qiu, Y. An, Z. Zhao, Y. Li, and Y. Zhou, "Catalytic synthesis of single-walled carbon nanotubes from coal gas by chemical vapor deposition method," *Fuel Processing Technology*, vol. 85, no. 8-10, pp. 913–920, 2004.

[40] Y. Li, X. B. Zhang, X. Y. Tao et al., "Single phase $MgMoO_4$ as catalyst for the synthesis of bundled multi-wall carbon nanotubes by CVD," *Carbon*, vol. 43, no. 6, pp. 1325–1328, 2005.

[41] A. Eftekhari, S. Manafi, and F. Moztarzadeh, "Catalytic chemical vapor deposition preparation of multi-wall carbon nanotubes with cone-like heads," *Chemistry Letters*, vol. 35, no. 1, pp. 138-139, 2006.

[42] E. Terrado, M. Redrado, E. Muñoz, W. K. Maser, A. M. Benito, and M. T. Martínez, "Aligned carbon nanotubes grown on alumina and quartz substrates by a simple thermal CVD process," *Diamond and Related Materials*, vol. 15, no. 4-8, pp. 1059–1063, 2006.

[43] G. S. B. McKee, C. P. Deck, and K. S. Vecchio, "Dimensional control of multi-walled carbon nanotubes in floating-catalyst CVD synthesis," *Carbon*, vol. 47, no. 8, pp. 2085–2094, 2009.

[44] Y. Shirazi, M. A. Tofighy, T. Mohammadi, and A. Pak, "Effects of different carbon precursors on synthesis of multi-wall carbon nanotubes: purification and functionalization," *Applied Surface Science*, vol. 257, no. 16, pp. 7359–7367, 2011.

[45] N. M. Mubarak, F. Yusof, and M. F. Alkhatib, "The production of carbon nanotubes using two-stage chemical vapor deposition and their potential use in protein purification," *Chemical Engineering Journal*, vol. 168, no. 1, pp. 461–469, 2011.

[46] K. Hata, N. Futaba Don, K. Mizuno, T. Namai, M. Yumura, and S. Iijima, "Water-assisted highly efficient synthesis of impurity-free single-walled carbon nanotubes," *Science*, vol. 306, no. 5700, pp. 1362–1364, 2004.

[47] R. L. Vander Wal and T. M. Ticich, "Comparative flame and furnace synthesis of single-walled carbon nanotubes," *Chemical Physics Letters*, vol. 336, no. 1-2, pp. 24–32, 2001.

[48] L. Yuan, K. Saito, W. Hu, and Z. Chen, "Ethylene flame synthesis of well-aligned multi-walled carbon nanotubes," *Chemical Physics Letters*, vol. 346, no. 1-2, pp. 23–28, 2001.

[49] R. L. Vander Wal, G. M. Berger, and L. J. Hall, "Single-walled carbon nanotube synthesis via a multi-stage flame configuration," *The Journal of Physical Chemistry B*, vol. 106, no. 14, pp. 3564–3567, 2002.

[50] A. V. Saveliev, W. Merchan-Merchan, and L. A. Kennedy, "Metal catalyzed synthesis of carbon nanostructures in an opposed flow methane oxygen flame," *Combustion and Flame*, vol. 135, no. 1-2, pp. 27–33, 2003.

[51] G. Woo Lee, J. Jurng, and J. Hwang, "Synthesis of carbon nanotubes on a catalytic metal substrate by using an ethylene inverse diffusion flame," *Carbon*, vol. 42, no. 3, pp. 682–685, 2004.

[52] J. Gore and A. Sane, "Flame synthesis of carbon nanotubes," *Carbon Nanotubes-Synthesis, Characterization, Applications*, vol. 1, p. 16801, 2011.

[53] S. K. Woo, Y. T. Hong, and O. C. Kwon, "Flame synthesis of carbon nanotubes using a double-faced wall stagnation flow burner," *Carbon*, vol. 47, no. 3, pp. 912–916, 2009.

[54] N. K. Memon, F. Xu, G. Sun, S. J. B. Dunham, B. H. Kear, and S. D. Tse, "Flame synthesis of carbon nanotubes and few-layer graphene on metal-oxide spinel powders," *Carbon*, vol. 63, pp. 478–486, 2013.

[55] D. Zhou, E. V. Anoshkina, L. Chow, and G. Chai, "Synthesis of carbon nanotubes by electrochemical deposition at room temperature," *Carbon*, vol. 44, no. 5, pp. 1013–1016, 2006.

[56] M. Johnson, J. Ren, M. Lefler et al., "Carbon nanotube wools made directly from CO_2 by molten electrolysis: value driven

pathways to carbon dioxide greenhouse gas mitigation," *Materials Today Energy*, vol. 5, pp. 230–236, 2017.

[57] Z. Li, G. Wang, W. Zhang, Z. Qiao, and H. Wu, "Carbon nanotubes synthesis from CO_2 based on the molten salts electrochemistry: effect of alkaline earth carbonate additives on the diameter of the carbon nanotubes," *Journal of the Electrochemical Society*, vol. 166, no. 10, pp. D415–D420, 2019.

[58] S.-H. Jeong, J.-H. Ko, J.-B. Park, and W. Park, "A sonochemical route to single-walled carbon nanotubes under ambient conditions," *Journal of the American Chemical Society*, vol. 126, no. 49, pp. 15982-15983, 2004.

[59] M. Raja and S. H. Ryu, "Synthesis of carbon nanotube through sonochemical process under ambient conditions," *Journal of Nanoscience and Nanotechnology*, vol. 9, no. 10, pp. 5940–5945, 2009.

[60] Z. Wang, L. Wang, and H. Wang, "PEG-mediated hydrothermal growth of single-crystal tellurium nanotubes," *Crystal Growth & Design*, vol. 8, no. 12, pp. 4415–4419, 2008.

[61] M. H. Razali, A. Ahmad, M. A. Azaman, and K. A. M. Amin, "Physicochemical properties of carbon nanotubes (CNT's) synthesized at low temperature using simple hydrothermal method," *International Journal of Applied Chemistry*, vol. 12, pp. 273–280, 2016.

[62] B. Kitiyanan, W. E. Alvarez, J. H. Harwell, and D. E. Resasco, "Controlled production of single-wall carbon nanotubes by catalytic decomposition of CO on bimetallic Co-Mo catalysts," *Chemical Physics Letters*, vol. 317, no. 3-5, pp. 497–503, 2000.

[63] J. Liu, Z. Jiang, H. Yu, and T. Tang, "Catalytic pyrolysis of polypropylene to synthesize carbon nanotubes and hydrogen through a two-stage process," *Polymer Degradation and Stability-POLYM DEGRAD STABIL*, vol. 96, no. 10, pp. 1711–1719, 2011.

[64] H. I. Abdel-Shafy and M. S. M. Mansour, "Solid waste issue: sources, composition, disposal, recycling, and valorization," *Egyptian Journal of Petroleum*, vol. 27, no. 4, pp. 1275–1290, 2018.

[65] V. K. Yadav, K. K. Yadav, V. Tirth et al., "Extraction of value-added minerals from various agricultural, industrial and domestic wastes," *Materials*, vol. 14, no. 21, p. 6333, 2021.

[66] K. Mugadza, A. Stark, P. G. Ndungu, and V. O. Nyamori, "Effects of ionic liquid and biomass sources on carbon nanotube physical and electrochemical properties," *Sustainability*, vol. 13, no. 5, p. 2977, 2021.

[67] X. Gao, X. Du, T. S. Mathis et al., "Maximizing ion accessibility in MXene-knotted carbon nanotube composite electrodes for high-rate electrochemical energy storage," *Nature Communications*, vol. 11, no. 1, p. 6160, 2020.

[68] A. Roquia, A. Khalfan Hamed Alhashmi, and B. Hamed Abdullah Alhasmi, "Synthesis and characterisation of carbon nanotubes from waste of Juglans regia (walnut) shells," *Fullerenes, Nanotubes, and Carbon Nanostructures*, vol. 29, no. 11, pp. 860–867, 2021.

[69] N. A. Fathy, A. H. Basta, and V. F. Lotfy, "4- Novel trends for synthesis of carbon nanostructures from agricultural wastes," in *Carbon Nanomaterials for Agri-Food and Environmental Applications*, K. A. Abd-Elsalam, Ed., pp. 59–74, Elsevier, 2020.

[70] K. Welsher, Z. Liu, S. P. Sherlock et al., "A route to brightly fluorescent carbon nanotubes for near-infrared imaging in mice," *Nature Nanotechnology*, vol. 4, no. 11, pp. 773–780, 2009.

[71] S. Mubarik, N. Qureshi, Z. Sattar et al., "Synthetic approach to rice waste-derived carbon-based nanomaterials and their applications," *Nano*, vol. 1, no. 3, pp. 109–159, 2021.

[72] P. Hidalgo, G. Coronado, A. Sánchez, and R. Hunter, "Agro-industrial waste as precursor source for carbon nanotubes (CNTs) synthesis using a new technical of solvent autoignition," *IOP Conference Series: Earth and Environmental Science*, vol. 503, no. 1, p. 012025, 2020.

[73] N. Haleem, Y. Jamal, S. N. Khan, M. A. Baig, M. Wahab, and X. Yang, "Synthesis of carbon nanotubes (CNTs) from poultry litter for removal of chromium (Cr (VI)) from wastewater," *Materials*, vol. 14, no. 18, p. 5195, 2021.

[74] S. Khawkomol, R. Neamchan, T. Thongsamer et al., "Potential of biochar derived from agricultural residues for sustainable management," *Sustainability*, vol. 13, no. 15, p. 8147, 2021.

[75] D. M. Salama, M. E. Abd El-Aziz, M. E. El-Naggar, E. A. Shaaban, and M. S. Abd El-Wahed, "Synthesis of an eco-friendly nanocomposite fertilizer for common bean based on carbon nanoparticles from agricultural waste biochar," *Pedosphere*, vol. 31, no. 6, pp. 923–933, 2021.

[76] A. Orbaek White, A. Hedayati, T. Yick et al., "On the use of carbon cables from plastic solvent combinations of polystyrene and toluene in carbon nanotube synthesis," *Nanomaterials (Basel)*, vol. 12, no. 1, p. 9, 2022.

[77] K. Li, H. Zhang, Y. Zheng, G. Yuan, Q. Jia, and S. Zhang, "Catalytic preparation of carbon nanotubes from waste polyethylene using FeNi bimetallic nanocatalyst," *Nanomaterials*, vol. 10, no. 8, p. 1517, 2020.

[78] R. Singh, V. Volli, L. Lohani, and M. K. Purkait, "Synthesis of carbon nanotubes from industrial wastes following alkali activation and film casting method," *Waste and Biomass Valorization*, vol. 11, no. 9, pp. 4957–4966, 2020.

[79] G. Smagulova, N. Yesbolov, B. Kaidar, N. Vassilyeva, N. Prikhodko, and Z. Mansurov, "Synthesis of carbon nanotubes from polymer waste," in *In Proceedings of Proceedings of the 5th World Congress on New Technologies (NewTech'19)*, Lisbon, Portugal, August 2019.

[80] P. T. Williams, "Hydrogen and carbon nanotubes from pyrolysis-catalysis of waste plastics: a review," *Waste and Biomass Valorization*, vol. 12, no. 1, pp. 1–28, 2021.

[81] A. Bazargan and G. McKay, "A review - Synthesis of carbon nanotubes from plastic wastes," *Chemical Engineering Journal*, vol. 195-196, pp. 377–391, 2012.

[82] C. Zhuo, *Synthesis of carbon nanotubes from waste polyethylene plastics*, Northeastern University. Boston, Massachusetts, 2009.

[83] C. Wu, M. A. Nahil, N. Miskolczi, J. Huang, and P. T. Williams, "Production and application of carbon nanotubes, as a co-product of hydrogen from the pyrolysis-catalytic reforming of waste plastic," *Process Safety and Environmental Protection*, vol. 103, pp. 107–114, 2016.

[84] G. T. Smagulova, N. Vassilyeva, B. B. Kaidar et al., "Recycling of low-density polyethylene waste for synthesis of carbon nanotubes," *Journal of Engineering Physics and Thermophysics*, vol. 94, no. 2, pp. 431–436, 2021.

[85] J. G. S. Moo, A. Veksha, W.-D. Oh et al., "Plastic derived carbon nanotubes for electrocatalytic oxygen reduction reaction:

effects of plastic feedstock and synthesis temperature," *Electrochemistry Communications*, vol. 101, pp. 11–18, 2019.

[86] A. Pattanshetti, N. Pradeep, V. Chaitra, and V. Uma, "Synthesis of multi-walled carbon nanotubes (MWCNTs) from plastic waste & analysis of garlic coated gelatin/MWCNTs nanocomposite films as food packaging material," *SN Applied Sciences*, vol. 2, no. 4, p. 730, 2020.

[87] P. K. Tripathi, S. Durbach, and N. J. Coville, "Synthesis of multi-walled carbon nanotubes from plastic waste using a stainless-steel CVD reactor as catalyst," *Nanomaterials (Basel)*, vol. 7, no. 10, p. 284, 2017.

[88] F. Ramzan, B. Shoukat, M. Y. Naz et al., "Single step microwaves assisted catalytic conversion of plastic waste into valuable fuel and carbon nanotubes," *Thermochimica Acta*, vol. 715, p. 179294, 2022.

[89] A. Bianco, K. Kostarelos, and M. Prato, "Applications of carbon nanotubes in drug delivery," *Current Opinion in Chemical Biology*, vol. 9, no. 6, pp. 674–679, 2005.

[90] N. Gupta, V. Yadav, and R. Patel, "A brief review of the essential role of nanovehicles for improving the therapeutic efficacy of pharmacological agents against tumours," *Current Drug Delivery*, vol. 19, no. 3, pp. 301–316, 2022.

[91] S. Huang, X. Du, M. Ma, and L. Xiong, "Recent progress in the synthesis and applications of vertically aligned carbon nanotube materials," *Nanotechnology Reviews*, vol. 10, no. 1, pp. 1592–1623, 2021.

[92] M. El Rhazi, S. Majid, M. Elbasri, F. E. Salih, L. Oularbi, and K. Lafdi, "Recent progress in nanocomposites based on conducting polymer: application as electrochemical sensors," *International Nano Letters*, vol. 8, no. 2, pp. 79–99, 2018.

[93] J. Foroughi, G. M. Spinks, D. Antiohos et al., "Highly conductive carbon nanotube-graphene hybrid yarn," *Advanced Functional Materials*, vol. 24, no. 37, pp. 5859–5865, 2014.

[94] J. Di, X. Wang, Y. Xing et al., "Dry-processable carbon nanotubes for functional devices and composites," *Small*, vol. 10, no. 22, pp. 4606–4625, 2014.

[95] H. S. Abbo, K. C. Gupta, N. G. Khaligh, and S. J. J. Titinchi, "Carbon nanomaterials for wastewater treatment," *ChemBioEng Reviews*, vol. 8, no. 5, pp. 463–489, 2021.

[96] A. M. Adam, H. A. Saad, A. A. Atta et al., "An environmentally friendly method for removing Hg(II), Pb(II), Cd(II) and Sn(II) heavy metals from wastewater using novel metal–carbon-based composites," *Crystals*, vol. 11, no. 8, p. 882, 2021.

[97] J. Khan, S. Ilyas, B. Akram et al., "Zno/NiO coated multiwalled carbon nanotubes for textile dyes degradation," *Arabian Journal of Chemistry*, vol. 11, no. 6, pp. 880–896, 2018.

[98] L. Jiang and L. Gao, "Fabrication and characterization of ZnO-coated multi-walled carbon nanotubes with enhanced photocatalytic activity," *Materials Chemistry and Physics*, vol. 91, no. 2-3, pp. 313–316, 2005.

[99] K. Welsher, S. P. Sherlock, and H. Dai, "Deep-tissue anatomical imaging of mice using carbon nanotube fluorophores in the second near-infrared window," *Proceedings of the National Academy of Sciences*, vol. 108, no. 22, pp. 8943–8948, 2011.

[100] R. Peng, X. S. Tang, and D. Li, "Detection of individual molecules and ions by carbon nanotube-based differential resistive pulse sensor," *Small*, vol. 14, no. 15, p. 1800013, 2018.

[101] J. Jeevanandam, A. Barhoum, Y. S. Chan, A. Dufresne, and M. K. Danquah, "Review on nanoparticles and nanostructured materials: history, sources, toxicity and regulations," *Beilstein Journal of Nanotechnology*, vol. 9, pp. 1050–1074, 2018.

[102] S. Sharma, P. Sudhakara, A. A. B. Omran, J. Singh, and R. A. Ilyas, "Recent trends and developments in conducting polymer nanocomposites for multifunctional applications," *Polymers*, vol. 13, no. 17, p. 2898, 2021.

[103] A. Al Rashid, S. A. Khan, S. G. Al-Ghamdi, and M. Koç, "Additive manufacturing of polymer nanocomposites: needs and challenges in materials, processes, and applications," *Journal of Materials Research and Technology*, vol. 14, pp. 910–941, 2021.

[104] C. Mondal, D. Ghosh, T. Aditya, A. K. Sasmal, and T. Pal, "Mn_3O_4 nanoparticles anchored to multiwall carbon nanotubes: a distinctive synergism for high-performance supercapacitors," *New Journal of Chemistry*, vol. 39, no. 11, pp. 8373–8380, 2015.

[105] A. Patole and G. Lubineau, "Carbon nanotubes with silver nanoparticle decoration and conductive polymer coating for improving the electrical conductivity of polycarbonate composites," *Carbon*, vol. 81, pp. 720–730, 2015.

[106] G. Kiani, H. Sheikhloie, and A. Rostami, "Highly enhanced electrical conductivity and thermal stability of polythiophene/single-walled carbon nanotubes nanocomposite," *Iranian Polymer Journal*, vol. 20, pp. 623–632, 2011.

[107] X. Yuan and Y. Wang, "Radial deformation of single-walled carbon nanotubes adhered to solid substrates and variations of energy: atomistic simulations and continuum analysis," *International Journal of Solids and Structures*, vol. 144, pp. 145–159, 2018.

[108] Y. Yin, C. Liu, and S. Fan, "Hybrid energy storage devices combining carbon-nanotube/polyaniline supercapacitor with lead-acid battery assembled through a "directly-inserted" method," *RSC Advances*, vol. 4, no. 50, pp. 26378–26382, 2014.

[109] X. Wang, K. Jiang, and G. Shen, "Flexible fiber energy storage and integrated devices: recent progress and perspectives," *Materials Today*, vol. 18, no. 5, pp. 265–272, 2015.

[110] S. Wang and J. Qiu, "Enhancing thermal conductivity of glass fiber/polymer composites through carbon nanotubes incorporation," *Composites Part B: Engineering*, vol. 41, no. 7, pp. 533–536, 2010.

[111] Q. Liao, Z. Liu, W. Liu, C. Deng, and N. Yang, "Extremely high thermal conductivity of aligned carbon nanotube-polyethylene composites," *Scientific Reports*, vol. 5, no. 1, p. 16543, 2015.

[112] K. Chu, H. Guo, C. Jia et al., "Thermal properties of carbon nanotube-copper composites for thermal management applications," *Nanoscale Research Letters*, vol. 5, no. 5, pp. 868–874, 2010.

[113] J. Kong, C. Y. Zhang, and X. Cheng, "Novel cu–Cr alloy matrix CNT composites with enhanced thermal conductivity," *Applied Physics A*, vol. 112, no. 3, pp. 631–636, 2013.

[114] J. E. Ellis, U. Green, D. C. Sorescu, Y. Zhao, and A. Star, "Indium oxide—single-walled carbon nanotube composite for ethanol sensing at room temperature," *The Journal of Physical Chemistry Letters*, vol. 6, no. 4, pp. 712–717, 2015.

[115] F. Mendoza, D. M. Hernández, V. Makarov, E. Febus, B. R. Weiner, and G. Morell, "Room temperature gas sensor based on tin dioxide-carbon nanotubes composite films," *Sensors and Actuators B: Chemical*, vol. 190, pp. 227–233, 2014.

[116] L. F. Mabena, S. Sinha Ray, S. D. Mhlanga, and N. J. Coville, "Nitrogen-doped carbon nanotubes as a metal catalyst support," *Applied Nanoscience*, vol. 1, no. 2, pp. 67–77, 2011.

[117] H. Cho, H. Joo, H. Kim, J.-E. Kim, K.-S. Kang, and J. Yoon, "Enhanced photocatalytic activity of TiO_2 nanotubes decorated with erbium and reduced graphene oxide," *Applied Surface Science*, vol. 565, p. 150459, 2021.

[118] M. Alsawat, T. Altalhi, K. Gulati, A. Santos, and D. Losic, "Synthesis of carbon nanotube–nanotubular titania composites by catalyst-free CVD process: insights into the formation mechanism and photocatalytic properties," *ACS Applied Materials & Interfaces*, vol. 7, pp. 28361–28368, 2015.

[119] H. T. Chung, J. H. Won, and P. Zelenay, "Active and stable carbon nanotube/nanoparticle composite electrocatalyst for oxygen reduction," *Nature Communications*, vol. 4, no. 1, pp. 1–5, 2013.

[120] S. H. Khan and V. K. Yadav, "Advanced oxidation processes for wastewater remediation: an overview," in *Removal of Emerging Contaminants Through Microbial Processes*, M. P. Shah, Ed., pp. 71–93, Springer, Singapore: Singapore, 2021.

[121] Y. Virendra Kumar and P. Priti Raj, "Fly ash properties and their applications as a soil ameliorant," in *Amelioration Technology for Soil Sustainability*, K. R. Ashok, Ed., pp. 59–89, IGI Global, Hershey, PA, USA, 2019.

[122] N. Sankararamakrishnan, M. Jaiswal, and N. Verma, "Composite nanofloral clusters of carbon nanotubes and activated alumina: an efficient sorbent for heavy metal removal," *Chemical Engineering Journal*, vol. 235, pp. 1–9, 2014.

[123] S.-Y. Jeon, J. Yun, Y. S. Lee, and H. I. Kim, "Removal of Cu(II) ions by alginate/carbon nanotube/maghemite composite magnetic beads," *Composite Magnetic Beads Carbon Letters*, vol. 11, no. 2, pp. 117–121, 2010.

[124] C. L. Chen, X. K. Wang, and M. Nagatsu, "Europium adsorption on multiwall carbon nanotube/iron oxide magnetic composite in the presence of polyacrylic acid," *Environmental Science & Technology*, vol. 43, no. 7, pp. 2362–2367, 2009.